

Nonlinear Dynamic Systems Parameterization Using Interval-Based Global Optimization: Computing Lipschitz Constants and Beyond

Sebastian A. Nugroho*, Ahmad F. Taha^{*,†}, and Vu Hoang[†]

Abstract—Hundreds of state-feedback and observer designs for nonlinear dynamic systems (NDS) have been proposed in the past three decades. The designs assume that NDS nonlinearity satisfies one of the following *function set classifications*: bounded Jacobian, Lipschitz continuity, one-sided Lipschitz, and quadratic inner-boundedness. These function sets are defined by *constant* scalars or matrices that bound NDS nonlinearities. These constants (i) depend on the NDS’ operating region, topology, and parameters and (ii) are used to design observer/controller gains. Unfortunately, there is a near-complete absence of algorithms to compute such bounding constants.

This paper investigates a combination of analytical and computational methods to compute such constants. First, and for each function set classification, we derive analytical expressions for these bounding constants through global maximization formulations. Second, we develop a scalable interval-based global maximization algorithms to numerically obtain the bounding constants. The algorithms come with performance guarantees. Third, we showcase the effectiveness of the proposed approaches to find the corresponding parameters on some NDS models for traffic networks, and synchronous generator models.

Keywords—Nonlinear systems, bounded Jacobian, Lipschitz continuous, one-sided Lipschitz, quadratic inner-boundedness, interval arithmetic, interval-based global optimization.

I. INTRODUCTION

CONSIDER nonlinear dynamic systems (NDS) of the form

$$\dot{x} = f(x, u), \quad y = h(x, u), \quad (1)$$

where $x, u, y, f(\cdot)$, and $h(\cdot)$ define the n states, m control inputs, p output measurements, state and output measurement model nonlinearities. NDS model (1) represents a wide range of systems such as transportation, water, and energy systems. In the past three decades, an abundance of Lyapunov-based methods have been developed to perform state/output-feedback control and robust state estimation for NDS (1). These methods often consider or assume that nonlinear dynamics in (1) belong to one of the following function sets of nonlinear functions: (a) *bounded Jacobian*, (b) *Lipschitz continuous*, (c) *one-sided Lipschitz*, (d) *quadratic inner-boundedness*, and (e) *quadratically bounded*. For example, $f(\cdot)$ is locally Lipschitz continuous in Ω if the following holds

$$\|f(x, u) - f(\hat{x}, u)\|_2 \leq \gamma_l \|x - \hat{x}\|_2,$$

for a $\gamma_l \geq 0$ and all $(x, u), (\hat{x}, u) \in \Omega$. Tab. I lists the mathematical definitions of the other function sets.

In this paper, we investigate NDS *parameterization*. That is, computing *constants* that bound these nonlinearities—we refer to these constants as *NDS parameters* (or just simply *parameters*). For instance, the nonnegative constant γ_l defines the Lipschitz continuity property in the above example. This parameterization is crucial as hundreds of observer/controller design are in fact relying on accurate values of these constants—see Tab. I. In what follows, we perform a brief review on how these function set classifications have been utilized in some observer/controller design literature.

In [1]–[3], observer designs for Lipschitz NDS through solving linear matrix inequalities (LMIs) or semi-definite programs (SDP) are proposed. As an alternative to tackle some limitations in Lipschitz-based observer, observers for one-sided Lipschitz and quadratically inner-bounded systems are developed in [4]–[6]. For bounded Jacobian systems, the corresponding observer designs are proposed in [7]–[9]. The authors in [10] use these Jacobian bounds to propose a new approach of observer design for Lipschitz nonlinear systems, which is then improved in [11] to increase scalability. As for controller and observer-based stabilization designs, the authors in [12], [13] develop feedback stabilization framework given for quadratic boundedness NDS nonlinearity. Not to be confused with quadratic inner-boundedness, quadratic boundedness is a drastically different function set; see Tab. I. More on that to follow. For Lipschitz NDS, observer-based control framework are proposed in [14]–[16]. Various robust \mathcal{H}_∞ control designs assuming one-sided Lipschitz and quadratically inner-bounded conditions are developed in [17]–[20].

Appendix A lists detailed formulations of several LMI- and SDP-based formulations for observer/controller designs for NDS classes in Tab. I. For example, considering Lipschitz NDS

$$\dot{x} = Ax + f(x, u), \quad y = Cx$$

and Lipschitz constant γ_l for $f(\cdot)$, solving the following LMI

$$\begin{bmatrix} A^T P + PA - YC - C^T Y^T + \kappa \gamma_l^2 I & P^T \\ P & -\kappa I \end{bmatrix} \prec 0$$

for matrix variables P, Y and $\kappa > 0$ yields an asymptotically stable estimation error through observer dynamics

$$\dot{\hat{x}} = A\hat{x} + f(\hat{x}, u) + L(y - C\hat{x})$$

with gain $L = P^{-1}Y$. Notice that the solution to the above LMI depends on the Lipschitz constant γ_l . Appendix A also lists some LMI/SDP formulations for other function sets beyond Lipschitz ones.

*Department of Electrical and Computer Engineering, The University of Texas at San Antonio, One UTSA Circle, San Antonio, TX 78249. Emails: sebastian.nugroho@my.utsa.edu, ahmad.taha@utsa.edu.

[†]Department of Mathematics, The University of Texas at San Antonio, One UTSA Circle, San Antonio, TX 78249. Email: duynguyenvu.hoang@utsa.edu.

This work is partially supported by the Valero Energy Corporation and the National Science Foundation (NSF) under Grant CMMI-1728629, CMMI-1917164, DMS-1614797, and DMS-1810687.

[‡]Corresponding author.

From the aforementioned literature, we realize that most of these observer/controller designs are posed as SDPs that incorporate constants characterizing the nonlinearities in NDS. As such, finding the tightest bounds and constants is crucial. For example, in the case for Lipschitz functions, a larger γ_l than the actual one can yield infeasible SDPs—thereby labeling the constant a *conservative* Lipschitz constant. On the contrary, if we approximate γ_l such that the value is below the actual one, there is a possibility that, due to the dynamical behavior of the system, the Lipschitz condition characterized by γ_l may be violated in certain points in Ω . In turn, this can lead to an unstable closed-loop system performance. Therefore, it is very important to obtain the tightest bounds that characterize $\mathbf{f}(\cdot)$ for Lipschitz function sets and beyond: the core objective of this work. This importance is not only needed in the context of state estimation/stabilization of NDS, but also in other domain such as neural networks [21].

We note the following: (i) All of the aforementioned studies solely focus on developing methods for observer/controller designs while assuming that the NDS belongs to one of the aforementioned function sets, rather than attempting to find or design algorithms to obtain bounding constants. (ii) The literature mostly focuses on small-scale dynamic systems where bounding constants can be obtained analytically. In fact, we have found that although analytical computations of Lipschitz constants can be useful, such computations could return large Lipschitz constants that are way too conservative [22]. Therefore, in order to be able to use these observer designs for a high-dimensional large-scale NDS, there is a need for systematic methods that are dedicated for NDS parameterization.

To the best of our knowledge, there are no computational methods in the literature that parameterize the nonlinearities in complex, large-scale NDS—beyond Lipschitz nonlinear systems. With that in mind, some recent studies have proposed methods to parameterize some Lipschitz NDS only. The authors in [23] propose a stochastic method to approximate Lipschitz constant, albeit only applicable for functions containing single variable. In [24], a method of computing Lipschitz constant for continuously differentiable real-valued function is presented. Recently, authors in [25] propose fast numerical methods for computing Lipschitz constant using interval arithmetic and automatic differentiation. A new approach to find a tight Lipschitz bounds based on SDP for feed-forward neural networks is proposed in [21], while authors in [26] employ *kernelized density estimation* to estimate Lipschitz constant using data generated from unknown dynamical systems. The majority of these works only focus on parameterizing one class of nonlinearity, that is, Lipschitz continuous. For the remaining function sets in Tab. I, no methodology has been put forth.

The objective of this work is to provide a framework for NDS parameterization for large-scale NDS via systematic methods to compute the corresponding constants/parameters for each class of aforementioned nonlinearities, considering arbitrary nonlinear models with continuous partial derivatives. These constants are computed by through optimally solving global maximization problem over a convex compact set through global optimization algorithms based on *interval arithmetic* (IA). The paper contributions are summarized as follows:

Table I
FUNCTION SETS OF NONLINEARITY CONSIDERED IN THIS PAPER.

Class	Mathematical Property
<i>Bounded Jacobian</i>	$-\infty < \underline{f}_{ij} \leq \frac{\partial f_i}{\partial x_j}(\mathbf{x}, \mathbf{u}) \leq \bar{f}_{ij} < +\infty,$ $(\mathbf{x}, \mathbf{u}) \in \Omega, \underline{f}_{ij}, \bar{f}_{ij} \in \mathbb{R}$
<i>Lipschitz Continuous</i>	$\ \mathbf{f}(\mathbf{x}, \mathbf{u}) - \mathbf{f}(\hat{\mathbf{x}}, \mathbf{u})\ _2 \leq \gamma_l \ \mathbf{x} - \hat{\mathbf{x}}\ _2$ $(\mathbf{x}, \mathbf{u}), (\hat{\mathbf{x}}, \mathbf{u}) \in \Omega, \gamma_l \in \mathbb{R}_+$
<i>One-Sided Lipschitz</i>	$\langle \mathbf{G}(\mathbf{f}(\mathbf{x}, \mathbf{u}) - \mathbf{f}(\hat{\mathbf{x}}, \mathbf{u})), \mathbf{x} - \hat{\mathbf{x}} \rangle \leq \gamma_s \ \mathbf{x} - \hat{\mathbf{x}}\ _2^2,$ $(\mathbf{x}, \mathbf{u}), (\hat{\mathbf{x}}, \mathbf{u}) \in \Omega, \gamma_s \in \mathbb{R}$
<i>Quadratically Inner-Bounded</i>	$\langle \mathbf{G}(\mathbf{f}(\mathbf{x}, \mathbf{u}) - \mathbf{f}(\hat{\mathbf{x}}, \mathbf{u})), \mathbf{G}(\mathbf{f}(\mathbf{x}, \mathbf{u}) - \mathbf{f}(\hat{\mathbf{x}}, \mathbf{u})) \rangle \leq$ $\gamma_{q1} \ \mathbf{x} - \hat{\mathbf{x}}\ _2^2 + \gamma_{q2} \langle \mathbf{G}(\mathbf{f}(\mathbf{x}, \mathbf{u}) - \mathbf{f}(\hat{\mathbf{x}}, \mathbf{u})), \mathbf{x} - \hat{\mathbf{x}} \rangle,$ $(\mathbf{x}, \mathbf{u}), (\hat{\mathbf{x}}, \mathbf{u}) \in \Omega, \gamma_{q1}, \gamma_{q2} \in \mathbb{R}$
<i>Quadratically Bounded</i>	$\langle \mathbf{f}(\mathbf{x}), \mathbf{f}(\mathbf{x}) \rangle \leq \mathbf{x}^\top \mathbf{\Gamma}^\top \mathbf{\Gamma} \mathbf{x},$ $\mathbf{x} \in \mathcal{X}, \mathbf{\Gamma} \in \mathbb{R}^{h \times n}$

- Proposing analytical formulations, posed as global maximization problems, to determine the corresponding constants that characterize the aforementioned function sets. It is demonstrated later that, using the proposed interval-based global maximization algorithm, this approach can be scalable for high-dimensional large-scale NDS since (a) we only need to solve optimization problems for each type of nonlinearities and (b) it is possible to consider a small portion of optimization variables.
- Investigating an interval-based global maximization algorithm designed specifically for computing the corresponding constants/parameters for the aforementioned function sets. This algorithm is based on IA and *branch-and-bound* (BnB) routines since it can provide tight lower and upper bounds for NDS parameters.
- Showcasing the effectiveness and applicability of the proposed framework for NDS parameterization as well as observer designs for different kinds of NDS including traffic networks, synchronous generator, and dynamics of a moving object.

A preliminary version of this work appears in [27], where we (i) discover a new relation between Lipschitz and quadratically inner-bounded function sets and (ii) pinpoint mistakes made in the numerical section of [6], [28] and present the appropriate corrections. The structure of this paper is described as follows. Section II showcases the problem formulation. In Section III, closed-form formulations to determine the corresponding constants for all function sets through global maximization problems are all presented. Section IV presents the proposed algorithms for global optimization based on IA designed specifically for solving problems given in Section III. Thorough numerical examples are provided in Section V and the paper is concluded in Section VI.

Notation Italicized, boldface upper and lower case characters represent matrices and column vectors: a is a scalar, \mathbf{a} is a vector, and \mathbf{A} is a matrix. Matrix \mathbf{I} denotes the identity square matrix, whereas \mathbf{O} denotes a zero matrix of appropriate dimensions. The notations \mathbb{N} , \mathbb{R} , \mathbb{R}_+ , and \mathbb{R}_{++} denote the set of natural, real, non-negative, and positive real numbers. The notations \mathbb{R}^n and $\mathbb{R}^{p \times q}$ denote the sets of row vectors with n elements and matrices with size p -by- q with elements in \mathbb{R} . For any vector $\mathbf{x} \in \mathbb{R}^n$, $\|\mathbf{x}\|_2$ denotes the Euclidean norm of \mathbf{x} , defined as $\|\mathbf{x}\|_2 := \sqrt{\mathbf{x}^\top \mathbf{x}}$, where \mathbf{x}^\top is the transpose of \mathbf{x} .

For $\mathbf{x}, \mathbf{y} \in \mathbb{R}^n$, inner product is defined as $\langle \mathbf{x}, \mathbf{y} \rangle := \mathbf{x}^\top \mathbf{y}$. If \mathbf{A} is a matrix, $\|\mathbf{A}\|_2$ denotes the induced 2-norm of \mathbf{A} and $A_{(i,j)}$ denotes its i -th and j -th element. The set $\mathbb{I}(n)$ is defined as $\mathbb{I}(n) := \{i \in \mathbb{N} \mid 1 \leq i \leq n\}$, which is usually used to represent the set of indices. The notions \mathbf{D}_x and ∇_x denote the Jacobian matrix and gradient vector with respect to vector \mathbf{x} . For a square matrix \mathbf{A} , $\lambda_{\max}(\mathbf{A})$ and $\lambda_{\min}(\mathbf{A})$ respectively return the maximum and minimum eigenvalues of \mathbf{A} . The set of all intervals containing real numbers is denoted by \mathbb{IR} , whereas n -dimensional intervals is denoted by \mathbb{IR}^n .

II. PROBLEM FORMULATION

In this paper, we consider any NDS of the following form

$$\dot{\mathbf{x}}(t) = \mathbf{A}\mathbf{x}(t) + \mathbf{G}\mathbf{f}(\mathbf{x}, \mathbf{u}) + \mathbf{B}\mathbf{u}(t), \quad (2)$$

where vectors $\mathbf{x} \in \mathcal{X} \subset \mathbb{R}^n$ and $\mathbf{u} \in \mathcal{U} \subset \mathbb{R}^m$ represent the state and input of the system, function $\mathbf{f} : \mathbb{R}^n \times \mathbb{R}^m \rightarrow \mathbb{R}^g$ captures any nonlinear phenomena, and $\mathbf{A}, \mathbf{B}, \mathbf{G}$ are known constant matrices of appropriate dimensions. For brevity, we drop the time dependence from now on such that $\mathbf{x} := \mathbf{x}(t)$; the same also applies to \mathbf{u} . We define $\Omega := \mathcal{X} \times \mathcal{U}$ with $\Omega \subset \mathbb{R}^p$ so that the domain of $\mathbf{f}(\cdot)$ can be simply referred to as Ω . The following assumptions are considered in this paper.

Assumption 1. *The conditions below apply to NDS (2)*

- 1) $\Omega := \prod_{i \in \mathbb{I}(n)} \Omega_i$ is a nonempty n -dimensional orthotope (may also be referred to as hyperrectangle or box). That is, $\Omega_i = [\underline{\omega}_i, \bar{\omega}_i]$ where $\underline{\omega}_i, \bar{\omega}_i \in \mathbb{R}$ are known bounds.
- 2) $\mathbf{f}(\cdot)$ is differentiable and has continuous partial derivatives in Ω .

The first assumption dictates that each x_i and u_j belongs to convex compact sets \mathcal{X}_i and \mathcal{U}_j respectively. This assumption is by not restrictive, seeing that cyber-physical systems have bounded states and inputs, where each upper and lower bounds define the operating regions. The second assumption ensures that the partial derivatives of $\mathbf{f}(\cdot)$ and hence its gradient vector $\nabla \mathbf{f}(\cdot)$ are bounded within the set Ω [29].

In this paper, we are interested in finding a way to parameterize the nonlinear function $\mathbf{f}(\cdot)$ into the function sets listed in Tab. I. This essentially boils down to computing the corresponding constants for each nonlinearity—this is referred to as *parameterization*. Assumption 1 allows $\mathbf{f}(\cdot)$ to be classified into any of these function sets since any $\mathbf{f}(\cdot)$ having continuous partial derivatives inside Ω has bounded Jacobian matrix, which implies Lipschitz continuous. As such, it may also be classified into one-sided Lipschitz and quadratically inner-bounded function sets [4]. As the consequence, one can utilize a plethora of observer/controller designs for NDS of the form (2). It is worthwhile mentioning that, since $(\mathbf{x}, \mathbf{u}) \in \Omega$, these function sets are valid *locally* (or *semi-global*) in the region of interest Ω .

To parameterize $\mathbf{f}(\cdot)$, first it is truly crucial to obtain well-defined formulations that allow the parameterization of these function sets to be performed effectively by employing optimization routines. The next section demonstrates how NDS parameterization can be posed as a global maximization problem over the set Ω .

III. SYNTHESIS OF GLOBAL MAXIMIZATION PROBLEMS FOR NDS PARAMETERIZATION

This section presents comprehensive formulations that pose the parameterization of $\mathbf{f}(\cdot)$ as global maximization problems in which the objective functions are all given in closed-form expressions, thereby making them applicable for the majority of deterministic global optimization algorithms.

A. Bounded Jacobian

Bounds for partial derivatives of $\mathbf{f}(\cdot)$ denoted by \underline{f}_{ij} and \bar{f}_{ij} for each $i \in \mathbb{I}(g)$ and $j \in \mathbb{I}(n)$ can be computed as

$$\bar{f}_{ij} = \max_{(\mathbf{x}, \mathbf{u}) \in \Omega} \frac{\partial f_i}{\partial x_j}(\mathbf{x}, \mathbf{u}) \quad (3a)$$

$$\underline{f}_{ij} = \min_{(\mathbf{x}, \mathbf{u}) \in \Omega} \frac{\partial f_i}{\partial x_j}(\mathbf{x}, \mathbf{u}) = - \max_{(\mathbf{x}, \mathbf{u}) \in \Omega} - \frac{\partial f_i}{\partial x_j}(\mathbf{x}, \mathbf{u}). \quad (3b)$$

Note that there is a chance for $\frac{\partial f_i}{\partial x_j}(\cdot)$ not to include each x_j and u_j . It is possible to speed up the computation in solving (3) by reducing the search space Ω to $\Omega_{r_i} := \mathcal{X}_{r_i} \times \mathcal{U}_{r'_i}$ where $\mathcal{X}_{r_i} = \prod_{j \in \mathbb{I}(r_i)} \mathcal{X}_j$ and $\mathcal{U}_{r'_i} = \prod_{j \in \mathbb{I}(r'_i)} \mathcal{U}_j$ such that every $x_j \in \mathcal{X}_j$ and $u_j \in \mathcal{U}_j$ are variables included in $\frac{\partial f_i}{\partial x_j}(\cdot)$.

Remark 1. *The reduction of Ω can also be applied for parameterizing other function sets whenever the objective function to be maximized does not include all variables from \mathbf{x} and \mathbf{u} . This potentially allows faster computational time as well as reduces the memory size required to perform the computation.*

B. Lipschitz Continuous

Since it is assumed that Assumption 1 holds for NDS (2), $\mathbf{f}(\cdot)$ always satisfies the Lipschitz continuity condition. Thus, the problem posed is determining the tightest Lipschitz constant for $\mathbf{f}(\cdot)$ that is still useful for observer/controller design. According to [30], [31], Lipschitz constant γ_l for such NDS is nothing but the maximum value of the norm of Jacobian matrix of $\mathbf{f}(\cdot)$ over the set Ω , that is

$$\gamma_l = \max_{(\mathbf{x}, \mathbf{u}) \in \Omega} \|\mathbf{D}_x \mathbf{f}(\mathbf{x}, \mathbf{u})\|_2. \quad (4)$$

Although (4) provides a straightforward method to compute γ_l , it is unfortunately difficult to obtain a closed-form expression of (4) due to the use of 2-norm for the Jacobian matrix. We note that having a closed-form formulation for γ_l is important as many deterministic global optimization methods necessitate the closed-form expression of the objective function. With that in mind, the following provides a closed-form formulation to compute γ_l , which is given in Theorem 1—the following *mean value theorem* and *key lemma* are presented beforehand due to its significant role in constructing this theorem.

Lemma 1 (Mean Value Theorem). *Let the function $f : \mathbb{R} \rightarrow \mathbb{R}$ be continuous on $[a, b]$ and differentiable on (a, b) for $a, b \in \mathbb{R}$. Then there exists $\bar{\tau} \in (a, b)$ such that*

$$\frac{df}{dx}(\bar{\tau}) = \frac{f(b) - f(a)}{b - a}.$$

The proof of Lemma 1 is available in [29]. The next lemma, deduced from the mean value theorem, plays a crucial role in obtaining various explicit bounds needed for transforming NDS parameterization as global maximization problems.

Lemma 2 (Key Lemma). Let $\mathbf{F} \in \mathbb{R}^{g \times g}$ be an arbitrary matrix and $\mathbf{w} \in \mathbb{R}^g$ and $\mathbf{x}, \hat{\mathbf{x}} \in \mathbb{R}^n, \mathbf{u} \in \mathbb{R}^m$ such that $(\mathbf{x}, \mathbf{u}) \in \Omega$. Then there exists a $\bar{\tau} \in (0, 1)$ such that

$$\langle \mathbf{F}(\mathbf{f}(\mathbf{x}, \mathbf{u}) - \mathbf{f}(\hat{\mathbf{x}}, \mathbf{u})), \mathbf{w} \rangle = \langle \Xi(\hat{\mathbf{x}} + \bar{\tau}(\mathbf{x} - \hat{\mathbf{x}}), \mathbf{u})(\mathbf{x} - \hat{\mathbf{x}}), \mathbf{w} \rangle. \quad (5a)$$

where $\Xi := \Xi(\mathbf{x}, \mathbf{u}) \in \mathbb{R}^{g \times n}$ is given by

$$\Xi_{(i,j)}(\mathbf{x}, \mathbf{u}) := \sum_{k \in \mathbb{I}(g)} F_{(i,k)} \frac{\partial f_k}{\partial x_j}(\mathbf{x}, \mathbf{u}). \quad (5b)$$

Proof. Let $(\mathbf{x}, \mathbf{u}), (\hat{\mathbf{x}}, \mathbf{u}) \in \Omega$. Define two functions $\phi : \mathbb{R} \rightarrow \mathbb{R}$ and $\mathbf{g} : \mathbb{R} \rightarrow \mathbb{R}^n$ as follows

$$\phi(\tau) := \langle \mathbf{F} \mathbf{f}(\mathbf{g}(\tau)), \mathbf{w} \rangle, \quad \mathbf{g}(\tau) := \hat{\mathbf{x}} + \tau(\mathbf{x} - \hat{\mathbf{x}}),$$

Note that due to the assumed convexity of Ω , $(\mathbf{g}(\tau), \mathbf{u})$ is contained in Ω for all $\tau \in [0, 1]$. Since $\phi(\cdot)$ is continuous on $[0, 1]$ and differentiable on $(0, 1)$, then according to mean value theorem there exists $\bar{\tau} \in (0, 1)$ such that

$$\frac{d\phi}{d\tau}(\bar{\tau}) = \frac{\phi(1) - \phi(0)}{1 - 0} = \phi(1) - \phi(0). \quad (6a)$$

The left-hand side of (6a) reads

$$\sum_{i \in \mathbb{I}(g)} \sum_{k \in \mathbb{I}(g)} F_{(i,k)} \frac{\partial f_k}{\partial x_j}(\mathbf{g}(\bar{\tau}), \mathbf{u})(x_j - \hat{x}_j)w_i,$$

yielding the conclusion of our lemma. \blacksquare

Using key lemma, we propose Lipschitz parameterization as global maximization problem in the following theorem.

Theorem 1. The nonlinear function $\mathbf{f} : \mathbb{R}^n \times \mathbb{R}^m \rightarrow \mathbb{R}^g$ in (2) is locally Lipschitz continuous in Ω such that for any $(\mathbf{x}, \mathbf{u}), (\hat{\mathbf{x}}, \mathbf{u}) \in \Omega$ the following condition holds

$$\|\mathbf{f}(\mathbf{x}, \mathbf{u}) - \mathbf{f}(\hat{\mathbf{x}}, \mathbf{u})\|_2 \leq \gamma_{l_1} \|\mathbf{x} - \hat{\mathbf{x}}\|_2, \quad (7a)$$

where γ_{l_1} can be obtained from solving the following problem

$$\gamma_{l_1} = \left(\max_{(\mathbf{x}, \mathbf{u}) \in \Omega} \sum_{i \in \mathbb{I}(g)} \|\nabla_x f_i(\mathbf{x}, \mathbf{u})\|_2^2 \right)^{1/2}. \quad (7b)$$

Proof. Applying Lemma 2 with $\mathbf{F} = \mathbf{I}$ and $\mathbf{w} := \mathbf{f}(\mathbf{x}, \mathbf{u}) - \mathbf{f}(\hat{\mathbf{x}}, \mathbf{u})$ yields

$$\Xi_{(i,j)}(\mathbf{x}, \mathbf{u}) := \frac{\partial f_i}{\partial x_j}(\mathbf{x}, \mathbf{u}),$$

and therefore the right-hand side of (5a) reads

$$\Psi := \sum_{i \in \mathbb{I}(g)} \sum_{j \in \mathbb{I}(n)} \frac{\partial f_i}{\partial x_j}(\hat{\mathbf{x}} + \bar{\tau}(\mathbf{x} - \hat{\mathbf{x}}), \mathbf{u})(x_j - \hat{x}_j)w_i.$$

We now proceed to estimate Ψ . By the applying the Cauchy-Schwarz inequality twice (first to the sum over j and then over i), one can verify that

$$\begin{aligned} |\Psi|^2 &\leq \left(\sum_{i \in \mathbb{I}(g)} \|\nabla_x f_i(\hat{\mathbf{x}} + \bar{\tau}(\mathbf{x} - \hat{\mathbf{x}}), \mathbf{u})\|_2 \|\mathbf{x} - \hat{\mathbf{x}}\|_2 w_i \right)^2 \\ &\leq \left(\sum_{i \in \mathbb{I}(g)} \|\nabla_x f_i(\hat{\mathbf{x}} + \bar{\tau}(\mathbf{x} - \hat{\mathbf{x}}), \mathbf{u})\|_2^2 \right) \|\mathbf{x} - \hat{\mathbf{x}}\|_2^2 \|\mathbf{w}\|_2^2 \\ &\leq \left(\max_{(\mathbf{x}, \mathbf{u}) \in \Omega} \sum_{i \in \mathbb{I}(g)} \|\nabla_x f_i(\mathbf{x}, \mathbf{u})\|_2^2 \right) \|\mathbf{x} - \hat{\mathbf{x}}\|_2^2 \|\mathbf{w}\|_2^2. \end{aligned}$$

Revisiting (5a), we see that we have just shown

$$|\langle \mathbf{f}(\mathbf{x}, \mathbf{u}) - \mathbf{f}(\hat{\mathbf{x}}, \mathbf{u}), \mathbf{w} \rangle|^2 \leq \gamma_{l_1}^2 \|\mathbf{x} - \hat{\mathbf{x}}\|_2^2 \|\mathbf{w}\|_2^2$$

Using our definition of $\mathbf{w} = \mathbf{f}(\mathbf{x}, \mathbf{u}) - \mathbf{f}(\hat{\mathbf{x}}, \mathbf{u})$ this reduces to

$$\|\mathbf{f}(\mathbf{x}, \mathbf{u}) - \mathbf{f}(\hat{\mathbf{x}}, \mathbf{u})\|_2^4 \leq \gamma_{l_1}^2 \|\mathbf{x} - \hat{\mathbf{x}}\|_2^2 \|\mathbf{f}(\mathbf{x}, \mathbf{u}) - \mathbf{f}(\hat{\mathbf{x}}, \mathbf{u})\|_2^2$$

which immediately implies (7a) provided that $\|\mathbf{w}\|_2^2 > 0$. In the case that $\|\mathbf{w}\|_2^2 = 0$, (7a) holds trivially, so this completes the proof of the theorem. \blacksquare

Since the closed-form expression of (7b) can be determined, unlike the one provided in (4), Lipschitz constant γ_{l_1} can be computed using any deterministic global optimization algorithms. Notice that when the domain of interest Ω is large and the function $\mathbf{f}(\cdot)$ is of high dimension, solving (7b) may take a significant amount of computational time. In this regard, it is possible to ‘split’ the maximization problem (7b) into several smaller sub-problems so that it may be solved in a distributed fashion, as described in the following corollary.

Corollary 1. The nonlinear function $\mathbf{f} : \mathbb{R}^n \times \mathbb{R}^m \rightarrow \mathbb{R}^g$ in (2) is locally Lipschitz continuous in Ω satisfying (7a) with Lipschitz constant

$$\gamma_{l_2} = \left(\sum_{i \in \mathbb{I}(g)} \max_{(\mathbf{x}, \mathbf{u}) \in \Omega} \|\nabla_x f_i(\mathbf{x}, \mathbf{u})\|_2^2 \right)^{1/2}. \quad (8)$$

Proof. Suppose that $(\mathbf{x}^*, \mathbf{u}^*) \in \Omega$ is defined as

$$(\mathbf{x}^*, \mathbf{u}^*) := \arg \max_{(\mathbf{x}, \mathbf{u}) \in \Omega} \sum_{i \in \mathbb{I}(g)} \|\nabla_x f_i(\mathbf{x}, \mathbf{u})\|_2^2.$$

For any $i \in \mathbb{I}(g)$ the following holds

$$\|\nabla_x f_i(\mathbf{x}^*, \mathbf{u}^*)\|_2^2 \leq \max_{(\mathbf{x}, \mathbf{u}) \in \Omega} \|\nabla_x f_i(\mathbf{x}, \mathbf{u})\|_2^2. \quad (9a)$$

Therefore, from (9a) it is easy to confirm that

$$\begin{aligned} \max_{(\mathbf{x}, \mathbf{u}) \in \Omega} \sum_{i \in \mathbb{I}(g)} \|\nabla_x f_i(\mathbf{x}, \mathbf{u})\|_2^2 &= \sum_{i \in \mathbb{I}(g)} \|\nabla_x f_i(\mathbf{x}^*, \mathbf{u}^*)\|_2^2 \\ &\leq \sum_{i \in \mathbb{I}(g)} \max_{(\mathbf{x}, \mathbf{u}) \in \Omega} \|\nabla_x f_i(\mathbf{x}, \mathbf{u})\|_2^2. \end{aligned} \quad (9b)$$

This shows that (8) is also a Lipschitz constant for (7a). \blacksquare

Note that (9b) implies $\gamma_{l_1} \leq \gamma_{l_2}$. That is, γ_{l_2} is potentially more conservative than γ_{l_1} albeit (8) can be solved individually for each $f_i(\cdot)$ to reduce computational time. This introduces trade-offs between (7b) and (8).

C. One-Sided Lipschitz

One-sided Lipschitz is another function set that is a generalization of Lipschitz continuity: a Lipschitz continuous function is also one-sided Lipschitz [4]. Realize that one-sided Lipschitz constant γ_s can be any real number while Lipschitz constant can only be nonnegative, as described in Tab. 1. The following example delineates this point.

Example 1. Consider the function $f : \mathbb{R} \rightarrow \mathbb{R}$ defined as

$$f(x) = -x^3 - 100x. \quad (10)$$

This function is globally one-sided Lipschitz with constant $\gamma_s = -100$. This can be seen from expanding the left-hand side of the one-sided Lipschitz condition described in Tab. 1

$$\begin{aligned} (f(x) - f(\hat{x}))(x - \hat{x}) &= (-x^3 + \hat{x}^3 - 100(x - \hat{x}))(x - \hat{x}) \\ &\leq -100(x - \hat{x})^2, \end{aligned}$$

which is due to $(-x^3 + \hat{x}^3)(x - \hat{x}) \leq 0$. On the other hand, an estimation of Lipschitz constant for $f(\cdot)$, say on the interval $\mathcal{X} = [-1, 1]$ would be at least equal to $\gamma_l = 103$. Thus, the sign information $\gamma_s < 0$ might give an advantage over γ_l in their application for observer design, as argued in [4]. Fig. 1 provides a simplistic illustration on function $f(\cdot)$ described in (10) with Lipschitz and one-sided Lipschitz conditions.

In this section, we derive numerical methods to compute one-sided Lipschitz constant γ_s for NDS of the form (2) so that it is possible to have $\gamma_s \in \mathbb{R}$. In this regard, first we propose numerical formulations that provide lower and upper bounds towards the left-hand side of one-sided Lipschitz condition presented in Tab. I, which is summarized in the following proposition.

Proposition 1. *For the nonlinear function $\mathbf{f} : \mathbb{R}^n \times \mathbb{R}^m \rightarrow \mathbb{R}^g$ in (2), there exist $\bar{\gamma}, \underline{\gamma} \in \mathbb{R}$ such that for any $(\mathbf{x}, \mathbf{u}), (\hat{\mathbf{x}}, \mathbf{u}) \in \Omega$ the following condition holds*

$$\underline{\gamma} \|\mathbf{x} - \hat{\mathbf{x}}\|_2^2 \leq \langle \mathbf{G}(\mathbf{f}(\mathbf{x}, \mathbf{u}) - \mathbf{f}(\hat{\mathbf{x}}, \mathbf{u})), \mathbf{x} - \hat{\mathbf{x}} \rangle \leq \bar{\gamma} \|\mathbf{x} - \hat{\mathbf{x}}\|_2^2, \quad (11a)$$

where $\bar{\gamma}$ and $\underline{\gamma}$ are given as

$$\bar{\gamma} = \max_{(\mathbf{x}, \mathbf{u}) \in \Omega} \lambda_{\max} \left(\frac{1}{2} (\Xi(\mathbf{x}, \mathbf{u}) + \Xi^\top(\mathbf{x}, \mathbf{u})) \right) \quad (11b)$$

$$\underline{\gamma} = \min_{(\mathbf{x}, \mathbf{u}) \in \Omega} \lambda_{\min} \left(\frac{1}{2} (\Xi(\mathbf{x}, \mathbf{u}) + \Xi^\top(\mathbf{x}, \mathbf{u})) \right), \quad (11c)$$

where each of the i -th and j -th element of $\Xi(\cdot)$ is specified as

$$\Xi_{(i,j)}(\mathbf{x}, \mathbf{u}) := \sum_{k \in \mathbb{I}(g)} G_{(i,k)} \frac{\partial f_k}{\partial x_j}(\mathbf{x}, \mathbf{u}). \quad (11d)$$

Proof. Applying key lemma with $\mathbf{w} := \mathbf{x} - \hat{\mathbf{x}}$, we get

$$\begin{aligned} & \langle \mathbf{G}(\mathbf{f}(\mathbf{x}, \mathbf{u}) - \mathbf{f}(\hat{\mathbf{x}}, \mathbf{u})), (\mathbf{x} - \hat{\mathbf{x}}) \rangle \\ &= (\mathbf{x} - \hat{\mathbf{x}})^\top \Xi^\top(\mathbf{z}, \mathbf{u}) (\mathbf{x} - \hat{\mathbf{x}}) \end{aligned} \quad (12)$$

where the matrix $\Xi(\cdot)$ in (12) is described in (11d) and $\mathbf{z} = \hat{\mathbf{x}} + \bar{\tau}(\mathbf{x} - \hat{\mathbf{x}})$ for some $\bar{\tau} \in [0, 1]$. Now (12) is equal to

$$(\mathbf{x} - \hat{\mathbf{x}})^\top \left(\frac{1}{2} (\Xi(\mathbf{z}, \mathbf{u}) + \Xi^\top(\mathbf{z}, \mathbf{u})) \right) (\mathbf{x} - \hat{\mathbf{x}}).$$

Since $\left(\frac{1}{2} (\Xi(\mathbf{z}, \mathbf{u}) + \Xi^\top(\mathbf{z}, \mathbf{u})) \right)$ is symmetric, we can apply the Rayleigh quotient [32] to obtain

$$\begin{aligned} \langle \mathbf{G}(\mathbf{f}(\mathbf{x}, \mathbf{u}) - \mathbf{f}(\hat{\mathbf{x}}, \mathbf{u})), \mathbf{x} - \hat{\mathbf{x}} \rangle &\leq \bar{\gamma} \|\mathbf{x} - \hat{\mathbf{x}}\|_2^2 \\ \langle \mathbf{G}(\mathbf{f}(\mathbf{x}, \mathbf{u}) - \mathbf{f}(\hat{\mathbf{x}}, \mathbf{u})), \mathbf{x} - \hat{\mathbf{x}} \rangle &\geq \underline{\gamma} \|\mathbf{x} - \hat{\mathbf{x}}\|_2^2, \end{aligned}$$

which establishes (11a) whilst $\bar{\gamma}$ and $\underline{\gamma}$ are equivalent to (11b) and (11c) respectively. ■

From Proposition 1, one-sided Lipschitz constant for NDS (2) is nothing but $\gamma_s = \bar{\gamma}$. This result generalizes the approach to compute one-sided Lipschitz constant in [4] in the sense that first, our result applies for a more general form of NDS expressed in (2) and second, we also obtain a lower bound for the left-hand side of one-sided Lipschitz condition presented in Tab. I, which is useful for determining quadratically inner-bounded constants, as later explained in the next section. Yet, the non closed-form expression for $\bar{\gamma}$ described in (11b) and similarly in [4] makes it difficult to compute via many deterministic global optimization methods. To that end, instead of solving (11b) we can choose to solve another problem that,

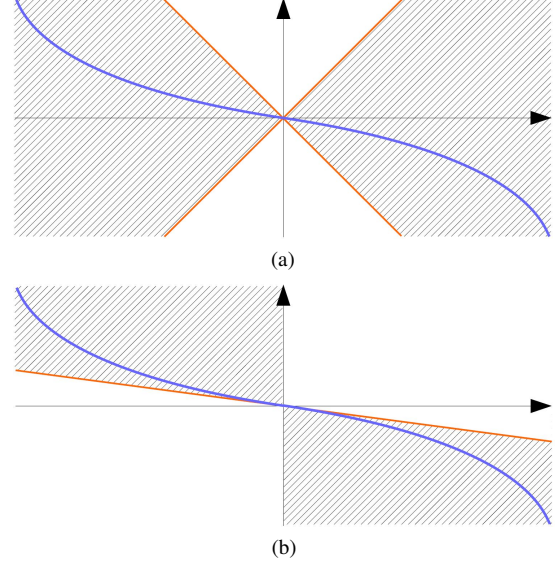


Figure 1. Since the function $f(x) = -x^3 - 100x$ (in blue) lies in the shaded area, then it satisfies two conditions: (a) Lipschitz continuous and (b) one-sided Lipschitz. Notice that the one-sided Lipschitz condition is characterized by a single straight line (in orange) having negative slope.

if successfully solved, produces an upper bound towards the solution of (11b). In what follows we discuss several solutions to this problem. First, a more direct conservative way to compute γ_s is proposed below.

Theorem 2. *The nonlinear function $\mathbf{f} : \mathbb{R}^n \times \mathbb{R}^m \rightarrow \mathbb{R}^g$ in (2) is one-sided Lipschitz continuous in Ω satisfying*

$$\langle \mathbf{G}(\mathbf{f}(\mathbf{x}, \mathbf{u}) - \mathbf{f}(\hat{\mathbf{x}}, \mathbf{u})), \mathbf{x} - \hat{\mathbf{x}} \rangle \leq \gamma_s \|\mathbf{x} - \hat{\mathbf{x}}\|_2^2 \quad (13a)$$

for all $(\mathbf{x}, \mathbf{u}), (\hat{\mathbf{x}}, \mathbf{u}) \in \Omega$ with

$$\gamma_s = \left(\max_{(\mathbf{x}, \mathbf{u}) \in \Omega} \sum_{i,j \in \mathbb{I}(g)} \left| \sum_{k \in \mathbb{I}(g)} G_{(i,k)} \frac{f_k}{x_j}(\mathbf{x}, \mathbf{u}) \right|^2 \right)^{1/2}. \quad (13b)$$

Proof. We simply find an upper bound for $\bar{\gamma}$ given in (11b). For fixed, but arbitrary $(\mathbf{x}, \mathbf{u}) \in \Omega$, let $\mathbf{v} \neq 0$ be an eigenvector for the maximal eigenvalue $\lambda_{\max}(\mathbf{x}, \mathbf{u})$ of $\frac{1}{2} (\Xi + \Xi^\top)$. From the eigenvalue equation and the fact that $\langle \Xi \mathbf{v}, \mathbf{v} \rangle = \langle \Xi^\top \mathbf{v}, \mathbf{v} \rangle$ we can deduce that

$$\lambda_{\max}(\mathbf{x}, \mathbf{u}) \|\mathbf{v}\|_2^2 = \langle \Xi(\mathbf{x}, \mathbf{u}) \mathbf{v}, \mathbf{v} \rangle$$

and hence

$$\lambda_{\max}(\mathbf{x}, \mathbf{u}) \|\mathbf{v}\|_2^2 \leq \|\Xi(\mathbf{x}, \mathbf{u})\|_2 \|\mathbf{v}\|_2^2. \quad (14)$$

To proceed, note that (13b) holds if $\bar{\gamma} \leq 0$. Otherwise, there is some point $(\mathbf{x}^*, \mathbf{u}^*)$ at which $\bar{\gamma} = \lambda_{\max}(\mathbf{x}^*, \mathbf{u}^*) > 0$. We can square (14) and recall the definition of $\Xi(\cdot)$ to get

$$\lambda_{\max}(\mathbf{x}^*, \mathbf{u}^*)^2 \leq \max_{(\mathbf{x}, \mathbf{u}) \in \Omega} \sum_{i,j \in \mathbb{I}(g)} \left| \sum_{k \in \mathbb{I}(g)} G_{(i,k)} \frac{f_k}{x_j}(\mathbf{x}, \mathbf{u}) \right|^2$$

and thus the desired result. ■

Another less straightforward, that is potentially less conservative approach to calculate γ_s than (13b) is to make use one of the consequence from *Gershgorin's circle theorem*. In essence, this particular theorem guarantees that each eigenvalue of a matrix

is always confined by a disk characterized by the diagonal and non-diagonal entries of that matrix [33]. The next proposition recapitulates this approach to compute an upper bound for the greatest eigenvalue of a symmetric matrix.

Proposition 2. *For any $\Psi \in \mathbb{S}^n$, the following inequality holds*

$$\lambda_{\max}(\Psi) \leq \max_{i \in \mathbb{I}(n)} \left(\Psi_{(i,i)} + \sum_{j \in \mathbb{I}(n) \setminus i} |\Psi_{(i,j)}| \right). \quad (15)$$

Proof. Suppose $\lambda \in \mathbb{R}$ be an eigenvalue of $\Psi \in \mathbb{S}^n$ and $\mathbf{v} \in \mathbb{R}^n$ be the corresponding eigenvector. Since $\mathbf{v} \neq \mathbf{0}$, then there exists v_i such that $|v_j| \leq |v_i|$ for all $j \in \mathbb{I}(n) \setminus i$. We then perform the following transformation: $\mathbf{v} \leftarrow \text{sgn}(v_i) \frac{\mathbf{v}}{|v_i|}$. Since the new \mathbf{v} also satisfies $(\Psi - \lambda \mathbf{I})\mathbf{v} = \mathbf{0}$, then at the i -th row we have

$$\lambda v_i = \sum_{j \in \mathbb{I}(n)} \Psi_{(i,j)} v_j = \Psi_{(i,i)} v_i + \sum_{j \in \mathbb{I}(n) \setminus i} \Psi_{(i,j)} v_j. \quad (16a)$$

Observe that the prior transformation leads to $v_i = 1$ and $|v_j| \leq 1$ for all $j \in \mathbb{I}(n) \setminus i$. Therefore, from (16a) and applying the triangle inequality, we obtain

$$\lambda - \Psi_{(i,i)} \leq \sum_{j \in \mathbb{I}(n) \setminus i} |\Psi_{(i,j)}| |v_j| \leq \sum_{j \in \mathbb{I}(n) \setminus i} |\Psi_{(i,j)}|. \quad (16b)$$

As (16b) applies to any eigenvalue of Ψ , then (15) holds. ■

Proposition 2 provides an amenable way which can be used for computing one-sided Lipschitz constant γ_s provided that $\Psi = \frac{1}{2} (\Xi(\mathbf{x}, \mathbf{u}) + \Xi^\top(\mathbf{x}, \mathbf{u}))$. That is,

$$\gamma_s = \max_{i \in \mathbb{I}(n)} \left(\max_{(\mathbf{x}, \mathbf{u}) \in \Omega} \left(\Psi_{(i,i)} + \sum_{j \in \mathbb{I}(n) \setminus i} |\Psi_{(i,j)}| \right) \right).$$

Note that in (15) it is possible for $\lambda_{\max}(\Psi)$ to be nonpositive assuming that Ψ is diagonally dominant with $\Psi_{(i,i)} \leq 0$ for each $i \in \mathbb{I}(n)$. In the following theorem, we develop an alternative method, aside from (15), to provide an upper bound for the greatest eigenvalue of any symmetric matrix.

Theorem 3. *It holds for any $\Psi \in \mathbb{S}^n$ that*

$$\lambda_{\max}(\Psi) \leq \max_{i \in \mathbb{I}(n)} \left(\Psi_{(i,i)} + \zeta_n \max_{j \in \mathbb{I}(n) \setminus i} |\Psi_{(i,j)}| \right), \quad (17a)$$

where $\zeta_n \in \mathbb{R}_{++}$ is a scalar that depends on the dimension n and is the optimal value of the following maximization problem

$$\zeta_n = \max_{\mathbf{v}} \frac{1}{v_i} - 1 \quad (17b)$$

$$\text{subject to } \sum_{j \in \mathbb{I}(n)} |v_j| = 1, \mathbf{v} \in \mathbb{R}^n \quad (17c)$$

$$v_i > 0, |v_j| \leq v_i, \forall j \in \mathbb{I}(n) \setminus i. \quad (17d)$$

Proof. Suppose $\lambda \in \mathbb{R}$ be an eigenvalue of $\Psi \in \mathbb{S}^n$ and $\mathbf{v} \in \mathbb{R}^n$ be the corresponding eigenvector. Since $\mathbf{v} \neq \mathbf{0}$, there exists v_i such that $|v_j| \leq |v_i|$ for every $j \in \mathbb{I}(n) \setminus i$. Next, the following transformation towards \mathbf{v} is applied

$$\mathbf{v} \leftarrow \text{sgn}(v_i) \frac{\mathbf{v}}{\sum_{j \in \mathbb{I}(n)} |v_j|}, \quad (18a)$$

where $\sum_{j \in \mathbb{I}(n)} |v_j| = 1$. As $(\Psi - \lambda \mathbf{I})\mathbf{v} = \mathbf{0}$ for such \mathbf{v} described in (18a), then at the i -th row we have

$$\lambda v_i = \sum_{j \in \mathbb{I}(n)} \Psi_{(i,j)} v_j = \Psi_{(i,i)} v_i + \sum_{j \in \mathbb{I}(n) \setminus i} \Psi_{(i,j)} v_j. \quad (18b)$$

Notice that the transformation (18a) yields $v_i > 0$ and $|v_j| \leq v_i$ for all $j \in \mathbb{I}(n) \setminus i$. Thus, from (18b) and applying the triangle inequality, we obtain

$$\begin{aligned} \lambda - \Psi_{(i,i)} &\leq \frac{1}{v_i} \left(\sum_{j \in \mathbb{I}(n) \setminus i} |\Psi_{(i,j)}| |v_j| \right) \\ &\leq \frac{1}{v_i} \left(\max_{j \in \mathbb{I}(n) \setminus i} |\Psi_{(i,j)}| \sum_{j \in \mathbb{I}(n) \setminus i} |v_j| \right) \\ &= \frac{\sum_{j \in \mathbb{I}(n) \setminus i} |v_j| - v_i}{v_i} \max_{j \in \mathbb{I}(n) \setminus i} |\Psi_{(i,j)}| \\ &= \left(\frac{1}{v_i} - 1 \right) \max_{j \in \mathbb{I}(n) \setminus i} |\Psi_{(i,j)}|. \end{aligned} \quad (18c)$$

Finally, since (18c) is valid for every eigenvalue of Ψ , then we eventually obtain (17a) where $\zeta_n = \frac{1}{v_i} - 1$ is computed through solving optimization problem specified in (17b)-(17d). ■

Note that finding ζ_n is a difficult task on its own since the optimization problem described in (17b)-(17d) has nonconvex objective function with nonconvex constraints. As such, we transform this problem into an equivalent convex one—summarized as follows.

Proposition 3. *The nonconvex maximization problem given in (17b)–(17d) is equivalent to the following convex problem*

$$v_i^* = \min_{\mathbf{v}, \mathbf{w} \in \mathbb{R}^n} v_i \quad (19a)$$

$$\text{subject to } \sum_{j \in \mathbb{I}(n)} w_j = 1, \quad (19b)$$

$$v_i > 0, w_j \leq v_i, \forall j \in \mathbb{I}(n) \setminus i. \quad (19c)$$

$$|v_i| = w_i, \forall i \in \mathbb{I}(n), \quad (19d)$$

where ζ_n in (17b) can be recovered from $\zeta_n^* = \frac{1}{v_i^*} - 1$.

In summary, this section proposes three different approaches to compute one-sided Lipschitz constant, all of which are based on computing an upper bound for the maximum eigenvalue of matrix $\Xi(\cdot)$. Define γ_{s1} , γ_{s2} , and γ_{s3} as one-sided Lipschitz constants obtained from (13b), (15), and (17a) respectively. Since Theorem 2 gives a nonnegative upper bound towards maximum eigenvalue, then in most cases we will likely have $\gamma_{s2} \leq \gamma_{s1}$ and $\gamma_{s3} \leq \gamma_{s1}$. However, further investigation is required to determine the relation between γ_{s2} and γ_{s3} .

D. Quadratic Inner-Boundedness

The concept of quadratic inner-boundedness has been extensively used alongside one-sided Lipschitz condition for a wide variety of observer design with applications ranging from state estimation to feedback stabilization [4], [6], [17]–[20]. Analogously to one-sided Lipschitz, the constants γ_{q1} and γ_{q2} for quadratically inner-bounded given in Tab. I may also be any real numbers. The following theorem summarizes our result for computing quadratically inner-bounded constants.

Theorem 4. *The nonlinear function $\mathbf{f} : \mathbb{R}^n \times \mathbb{R}^m \rightarrow \mathbb{R}^g$ in (2) is locally quadratically inner-bounded in Ω such that for any $(\mathbf{x}, \mathbf{u}), (\hat{\mathbf{x}}, \mathbf{u}) \in \Omega$ the following holds*

$$\langle \mathbf{G}(\mathbf{f}(\mathbf{x}, \mathbf{u}) - \mathbf{f}(\hat{\mathbf{x}}, \mathbf{u})), \mathbf{G}(\mathbf{f}(\mathbf{x}, \mathbf{u}) - \mathbf{f}(\hat{\mathbf{x}}, \mathbf{u})) \rangle \leq$$

$$\gamma_{q1}\|\mathbf{x} - \hat{\mathbf{x}}\|_2^2 + \gamma_{q2}\langle \mathbf{G}(\mathbf{f}(\mathbf{x}, \mathbf{u}) - \mathbf{f}(\hat{\mathbf{x}}, \mathbf{u})), \mathbf{x} - \hat{\mathbf{x}} \rangle, \quad (20a)$$

where for $\epsilon_1, \epsilon_2 \in \mathbb{R}_+$, $\gamma_{q2} = \epsilon_2 - \epsilon_1$ and γ_{q1} is specified as

$$\gamma_{q1} = \epsilon_1 \bar{\gamma} - \epsilon_2 \underline{\gamma} + \max_{(\mathbf{x}, \mathbf{u}) \in \Omega} \sum_{i \in \mathbb{I}(n)} \|\nabla_x \xi_i(\mathbf{x}, \mathbf{u})\|_2^2, \quad (20b)$$

where $\xi_i(\mathbf{x}, \mathbf{u}) := \sum_{j \in \mathbb{I}(g)} G_{(i,j)} f_j(\mathbf{x}, \mathbf{u})$ for $i \in \mathbb{I}(n)$ and $\bar{\gamma}$ and $\underline{\gamma}$ are the optimal values of (11b) and (11c).

Proof. Applying again Lemma 2 with $\mathbf{w} = \mathbf{G}(\mathbf{f}(\mathbf{x}, \mathbf{u}) - \mathbf{f}(\hat{\mathbf{x}}, \mathbf{u}))$, we can deduce the following result

$$\langle \mathbf{G}(\mathbf{f}(\mathbf{x}, \mathbf{u}) - \mathbf{f}(\hat{\mathbf{x}}, \mathbf{u})), \mathbf{G}(\mathbf{f}(\mathbf{x}, \mathbf{u}) - \mathbf{f}(\hat{\mathbf{x}}, \mathbf{u})) \rangle \leq \left(\max_{(\mathbf{x}, \mathbf{u}) \in \Omega} \sum_{i \in \mathbb{I}(n)} \|\nabla_x \xi_i(\mathbf{x}, \mathbf{u})\|_2^2 \right) \|\mathbf{x} - \hat{\mathbf{x}}\|_2^2. \quad (21a)$$

For brevity, we temporarily denote the above expression in round brackets by k . From (11a), we get for $\epsilon_1, \epsilon_2 \in \mathbb{R}_+$

$$0 \leq \epsilon_1 \bar{\gamma} \|\mathbf{x} - \hat{\mathbf{x}}\|_2^2 - \epsilon_1 \langle \mathbf{G}(\mathbf{f}(\mathbf{x}, \mathbf{u}) - \mathbf{f}(\hat{\mathbf{x}}, \mathbf{u})), \mathbf{x} - \hat{\mathbf{x}} \rangle \quad (21b)$$

$$0 \leq -\epsilon_2 \underline{\gamma} \|\mathbf{x} - \hat{\mathbf{x}}\|_2^2 + \epsilon_2 \langle \mathbf{G}(\mathbf{f}(\mathbf{x}, \mathbf{u}) - \mathbf{f}(\hat{\mathbf{x}}, \mathbf{u})), \mathbf{x} - \hat{\mathbf{x}} \rangle. \quad (21c)$$

Combine these two inequalities by multiplying both with (-1) and adding them to

$$-(\epsilon_2 - \epsilon_1) \langle \mathbf{G}(\mathbf{f}(\mathbf{x}, \mathbf{u}) - \mathbf{f}(\hat{\mathbf{x}}, \mathbf{u})), \mathbf{x} - \hat{\mathbf{x}} \rangle - (\epsilon_1 \bar{\gamma} - \epsilon_2 \underline{\gamma}) \|\mathbf{x} - \hat{\mathbf{x}}\|_2^2 \leq 0 \quad (21d)$$

Finally, we can deduce (20a) by using (21a), (21d) and noting that $k\|\mathbf{x} - \hat{\mathbf{x}}\|_2^2$ equals

$$\begin{aligned} & k\|\mathbf{x} - \hat{\mathbf{x}}\|_2^2 + (\epsilon_2 \underline{\gamma} - \epsilon_1 \bar{\gamma}) \langle \mathbf{G}(\mathbf{f}(\mathbf{x}, \mathbf{u}) - \mathbf{f}(\hat{\mathbf{x}}, \mathbf{u})), \mathbf{x} - \hat{\mathbf{x}} \rangle \\ & + (\epsilon_1 \bar{\gamma} - \epsilon_2 \underline{\gamma}) \langle \mathbf{G}(\mathbf{f}(\mathbf{x}, \mathbf{u}) - \mathbf{f}(\hat{\mathbf{x}}, \mathbf{u})), \mathbf{x} - \hat{\mathbf{x}} \rangle \\ & \leq \gamma_{q1} \|\mathbf{x} - \hat{\mathbf{x}}\|_2^2 + (\epsilon_2 \underline{\gamma} - \epsilon_1 \bar{\gamma}) \langle \mathbf{G}(\mathbf{f}(\mathbf{x}, \mathbf{u}) - \mathbf{f}(\hat{\mathbf{x}}, \mathbf{u})), \mathbf{x} - \hat{\mathbf{x}} \rangle \end{aligned}$$

with γ_{q1} given in (20b). ■

This result allows the quadratically inner-bounded constants γ_{q1} and γ_{q2} to be parametrized with nonnegative variables ϵ_1 and ϵ_2 , hence giving one kind of degree of freedom that can be useful for observer/controller design. From (21a) and using a similar approach as in Corollary 1, one can also verify that

$$\max_{(\mathbf{x}, \mathbf{u}) \in \Omega} \sum_{i \in \mathbb{I}(n)} \|\nabla_x \xi_i(\mathbf{x}, \mathbf{u})\|_2^2 \leq \sum_{i \in \mathbb{I}(n)} \max_{(\mathbf{x}, \mathbf{u}) \in \Omega} \|\nabla_x \xi_i(\mathbf{x}, \mathbf{u})\|_2^2,$$

which prospectively allows γ_{q1} to be computed more efficiently in a distributive manner.

E. Quadratic Boundedness

Unlike the other function sets, quadratic boundedness condition is mainly utilized to generate conditions for designing stabilizing feedback control actions, with a much less common applications in observer design [34]. This condition is introduced in [12] and has been widely applied since then for numerous stabilization purposes [13]. Following [12], [13], the subsequent assumptions towards $\mathbf{f}(\cdot)$ are considered: $\mathbf{f}(\cdot)$ is independent of \mathbf{u} and $\mathbf{f}(0) = 0$. As such the following result is established.

Theorem 5. The nonlinear function $\mathbf{f} : \mathbb{R}^n \rightarrow \mathbb{R}^g$ in (2) is locally quadratically bounded in \mathcal{X} so that for $\mathbf{x} \in \mathcal{X}$ we have

$$\langle \mathbf{f}(\mathbf{x}), \mathbf{f}(\mathbf{x}) \rangle \leq \mathbf{x}^\top \mathbf{\Gamma}^\top \mathbf{\Gamma} \mathbf{x}, \quad (22a)$$

where $\mathbf{\Gamma} \in \mathbb{R}^{n \times n}$ can be computed as follow

$$\mathbf{\Gamma} = \text{Diag} \left(\left\{ \max_{\mathbf{x} \in \mathcal{X}} \sqrt{n \sum_{i \in \mathbb{I}(g)} \left(\frac{\partial f_i}{\partial x_j}(\mathbf{x}) \right)^2} \right\}_{j=1}^n \right). \quad (22b)$$

Proof. Let $\mathbf{x}, \hat{\mathbf{x}} \in \mathcal{X}$ and define two functions $\phi : \mathbb{R} \rightarrow \mathbb{R}$ and $\mathbf{g} : \mathbb{R} \rightarrow \mathbb{R}^n$ as follows

$$\phi(\tau) := \langle \mathbf{f}(\mathbf{x}) - \mathbf{f}(\hat{\mathbf{x}}), \mathbf{f}(\mathbf{g}(\tau)) \rangle, \quad \mathbf{g}(\tau) := \hat{\mathbf{x}} + \tau(\mathbf{x} - \hat{\mathbf{x}}).$$

Since $\phi(\cdot)$ is continuous on $[0, 1]$ and differentiable on $(0, 1)$, then from mean value theorem there exists such $\bar{\tau} \in (0, 1)$ that

$$\frac{d\phi}{d\tau}(\bar{\tau}) = \frac{\phi(1) - \phi(0)}{1 - 0} = \phi(1) - \phi(0). \quad (23a)$$

For brevity, define $\tilde{\mathbf{f}}(\mathbf{x}, \hat{\mathbf{x}}) := \mathbf{f}(\mathbf{x}) - \mathbf{f}(\hat{\mathbf{x}})$. The left-hand side of (23a) is equivalent to

$$\begin{aligned} \frac{d\phi}{d\tau}(\bar{\tau}) &= \sum_{i \in \mathbb{I}(g)} \tilde{f}_i(\mathbf{x}, \hat{\mathbf{x}}) \frac{df_i(\mathbf{g}(\bar{\tau}))}{d\tau} \\ &= \sum_{i \in \mathbb{I}(g)} \tilde{f}_i(\mathbf{x}, \hat{\mathbf{x}}) \left(\sum_{j \in \mathbb{I}(n)} \frac{\partial f_i(\mathbf{g}(\bar{\tau}))}{\partial g_j} \cdot \frac{dg_j}{d\tau} \right). \end{aligned} \quad (23b)$$

Since $\frac{dg_j}{d\tau} = x_j - \hat{x}_j$ and $\mathbf{g}(\bar{\tau}) \in (\hat{\mathbf{x}}, \mathbf{x})$ for which $\bar{\tau} \in (0, 1)$ implies that there exists $\mathbf{z} \in (\hat{\mathbf{x}}, \mathbf{x})$, (23b) is equivalent to

$$\frac{d\phi}{d\tau}(\bar{\tau}) = \sum_{i \in \mathbb{I}(g)} \tilde{f}_i(\mathbf{x}, \hat{\mathbf{x}}) \left(\sum_{j \in \mathbb{I}(n)} \frac{\partial f_i(\mathbf{z})}{\partial x_j} (x_j - \hat{x}_j) \right). \quad (23c)$$

By realizing that the right hand side of (23a) is nothing but

$$\phi(1) - \phi(0) = \langle \tilde{\mathbf{f}}(\mathbf{x}, \hat{\mathbf{x}}), \mathbf{f}(\mathbf{g}(1)) - \mathbf{f}(\mathbf{g}(0)) \rangle = \|\tilde{\mathbf{f}}(\mathbf{x}, \hat{\mathbf{x}})\|_2^2,$$

then from the above, (23a), and (23c), one can verify that

$$\begin{aligned} \|\tilde{\mathbf{f}}(\mathbf{x}, \hat{\mathbf{x}})\|_2^2 &= \sum_{i \in \mathbb{I}(g)} \tilde{f}_i(\mathbf{x}, \hat{\mathbf{x}}) \left(\sum_{j \in \mathbb{I}(n)} \frac{\partial f_i(\mathbf{z})}{\partial x_j} (x_j - \hat{x}_j) \right) \\ &\leq \sum_{i \in \mathbb{I}(g)} \left| \tilde{f}_i(\mathbf{x}, \hat{\mathbf{x}}) \left(\sum_{j \in \mathbb{I}(n)} \frac{\partial f_i(\mathbf{z})}{\partial x_j} (x_j - \hat{x}_j) \right) \right| \\ &\leq \|\tilde{\mathbf{f}}(\mathbf{x}, \hat{\mathbf{x}})\|_2 \left(\sum_{i \in \mathbb{I}(g)} \left| \sum_{j \in \mathbb{I}(n)} \frac{\partial f_i(\mathbf{z})}{\partial x_j} (x_j - \hat{x}_j) \right|^2 \right)^{1/2}, \end{aligned}$$

from which we can imply that

$$\begin{aligned} \tilde{\mathbf{f}}(\mathbf{x}, \hat{\mathbf{x}})^\top \tilde{\mathbf{f}}(\mathbf{x}, \hat{\mathbf{x}}) &\leq \sum_{i \in \mathbb{I}(g)} \left| \sum_{j \in \mathbb{I}(n)} \frac{\partial f_i(\mathbf{z})}{\partial x_j} (x_j - \hat{x}_j) \right|^2 \\ &\leq \sum_{i \in \mathbb{I}(g)} \left(\sum_{j \in \mathbb{I}(n)} \left| \frac{\partial f_i(\mathbf{z})}{\partial x_j} (x_j - \hat{x}_j) \right| \right)^2 \\ &\leq \sum_{i \in \mathbb{I}(g)} n \left(\sum_{j \in \mathbb{I}(n)} \left(\frac{\partial f_i(\mathbf{z})}{\partial x_j} \right)^2 (x_j - \hat{x}_j)^2 \right) \\ &\leq \max_{\mathbf{x} \in \mathcal{X}} \sum_{i \in \mathbb{I}(g)} \sum_{j \in \mathbb{I}(n)} n \left(\frac{\partial f_i(\mathbf{x})}{\partial x_j} \right)^2 (x_j - \hat{x}_j)^2 \\ &\leq \sum_{j \in \mathbb{I}(n)} \left(\max_{\mathbf{x} \in \mathcal{X}} \sum_{i \in \mathbb{I}(g)} n \left(\frac{\partial f_i(\mathbf{x})}{\partial x_j} \right)^2 \right) (x_j - \hat{x}_j)^2 \\ &= (\mathbf{x} - \hat{\mathbf{x}})^\top \mathbf{\Gamma}^\top \mathbf{\Gamma} (\mathbf{x} - \hat{\mathbf{x}}), \end{aligned} \quad (23d)$$

where the diagonal matrix $\mathbf{\Gamma}$ is described in (22b). Since $\mathbf{f}(0) = 0$, then from (23d) one can immediately obtain (22a). ■

As seen in (22b), the matrix $\mathbf{\Gamma}$ is diagonal. As such, one can indeed solve the global maximization problem for each diagonal entry of $\mathbf{\Gamma}$ individually in a distributive manner without trading computational time with conservativeness.

Remark 2. (Difference between QB and QIB) Although the last two function sets—quadratic boundedness (QB) and quadratic inner-boundedness (QIB)—seemingly share canny resemblance due to their terminology, the two sets are drastically different. Admittedly, the terminology is somewhat confusing since it suggests a connection between the two. QB is simply a bound on the values the function can attain, implying that the norm of $\mathbf{f}(\cdot)$ is bounded by a quadratic function. On the other hand, QIB is akin to the Lipschitz condition, since it compares the values of $\mathbf{f}(\cdot)$ at two different points.

Tab. II provides a summary on the proposed global maximization problems for parameterizing NDS into bounded Jacobian, Lipschitz continuous, one-sided Lipschitz, quadratically inner-bounded, and quadratically bounded function sets given in Section III.

F. Discussion and New Insights

So far we have presented systematic methods of transforming NDS parameterization as global maximization problems for various function sets. It is worth noting that, for NDS having nonlinearities satisfy Assumption 1, this allows us to utilize a plethora of observer/controller designs from the literature. Indeed, the majority of these observer/controller are designed for specific function sets, such as bounded Jacobian [7], [9], [11], Lipschitz continuous [1], [2], [10], [14]–[16], [35], one-sided Lipschitz with quadratically inner-bounded [4]–[6], [17]–[20], and quadratically bounded [12], [13], [36].

In this section, we evaluate the understanding on the relation particularly between Lipschitz continuous and quadratically inner-bounded function sets and provide some necessary corrections. It is widely known that, given $\mathbf{G} = \mathbf{I}$ and $\mathbf{f}(\cdot)$ is Lipschitz continuous with Lipschitz constant γ_l , then $\mathbf{f}(\cdot)$ is also quadratically inner-bounded with $\gamma_{q1} = \gamma_l^2$ and $\gamma_{q2} = 0$ [28]. It is claimed in [28], however, that the converse does not hold in general. The following statement is remarked in that paper: if $\mathbf{f}(\cdot)$ is OSL and QIB with γ_{q2} positive, then $\mathbf{f}(\cdot)$ is Lipschitz continuous. Our investigation reveals that if a function $\mathbf{f}(\cdot)$ is QIB then it is *necessarily* Lipschitz continuous. This finding is summarized in the following theorem.

Theorem 6. Suppose that $\mathbf{f}(\cdot)$ is QIB with constants $\gamma_{q1}, \gamma_{q2} \in \mathbb{R}$ and $\mathbf{G} = \mathbf{I}$. Then, $\mathbf{f}(\cdot)$ is also Lipschitz continuous where the constants γ_{q1}, γ_{q2} necessarily satisfy the inequality

$$2\gamma_{q1} + |\gamma_{q2}|^2 \geq 0. \quad (24)$$

The above result—proven in [27]—suggests that quadratically inner-bounded implies Lipschitz continuity. Moreover since Lipschitz continuity implies quadratically inner-bounded, it can be concluded that both class of functions are the same. In fact, for given quadratically inner-bounded constants γ_{q1}, γ_{q2} , the corresponding Lipschitz constant can be computed as $\gamma_l = \sqrt{2\gamma_{q1} + |\gamma_{q2}|^2}$. Note that the condition (24) is necessary,

Table II
A SUMMARY OF NDS PARAMETERIZATION POSED AS GLOBAL MAXIMIZATION PROBLEMS.

Class	Parameter as Global Maximization Problem
Bounded Jacobian	$\bar{f}_{ij} = \max_{(\mathbf{x}, \mathbf{u}) \in \Omega} \frac{\partial f_i}{\partial x_j}(\mathbf{x}, \mathbf{u}),$ $\underline{f}_{ij} = -\max_{(\mathbf{x}, \mathbf{u}) \in \Omega} -\frac{\partial f_i}{\partial x_j}(\mathbf{x}, \mathbf{u})$
Lipschitz Continuous	$\gamma_{l1} = \left(\max_{(\mathbf{x}, \mathbf{u}) \in \Omega} \sum_{i \in \mathbb{I}(g)} \ \nabla_x f_i(\mathbf{x}, \mathbf{u})\ _2^2 \right)^{1/2},$ $\gamma_{l2} = \left(\sum_{i \in \mathbb{I}(g)} \max_{(\mathbf{x}, \mathbf{u}) \in \Omega} \ \nabla_x f_i(\mathbf{x}, \mathbf{u})\ _2^2 \right)^{1/2}$
One-Sided Lipschitz	$\gamma_{s1} = \left(\max_{(\mathbf{x}, \mathbf{u}) \in \Omega} \sum_{i, j \in \mathbb{I}(g)} \sigma(i, j) ^2 \right)^{1/2},$ $\sigma(i, j) := \sum_{k \in \mathbb{I}(g)} G_{(i, k)} \frac{f_k}{x_j}(\mathbf{x}, \mathbf{u}),$ $\gamma_{s2} = \gamma_{s3} = \max_{i \in \mathbb{I}(n)} \left(\max_{(\mathbf{x}, \mathbf{u}) \in \Omega} \psi(i) \right),$ $\psi(i) := \begin{cases} \Psi(i, i) + \sum_{j \in \mathbb{I}(n) \setminus i} \Psi(i, j) , & \text{for } \gamma_{s2} \\ \Psi(i, i) + \zeta_n \max_{j \in \mathbb{I}(n) \setminus i} \Psi(i, j) , & \text{for } \gamma_{s3} \end{cases}$ $\Psi = \frac{1}{2} (\Xi(\mathbf{x}, \mathbf{u}) + \Xi^T(\mathbf{x}, \mathbf{u})), \Xi \text{ defined in (11d)}$
Quadratically Inner-Bounded	$\gamma_{q1} = \epsilon_1 \bar{\gamma} - \epsilon_2 \underline{\gamma} + \max_{(\mathbf{x}, \mathbf{u}) \in \Omega} \sum_{i \in \mathbb{I}(n)} \ \nabla_x \xi_i(\mathbf{x}, \mathbf{u})\ _2^2,$ $\bar{\gamma} \text{ and } \underline{\gamma} \text{ given in (11b) and (11c),}$ $\gamma_{q2} = \epsilon_2 - \epsilon_1 \text{ where } \epsilon_1, \epsilon_2 \in \mathbb{R}_+,$
Quadratically Bounded	$\mathbf{\Gamma} = \text{Diag} \left(\left\{ \max_{\mathbf{x} \in \mathcal{X}} \sqrt{n \sum_{i \in \mathbb{I}(g)} \left(\frac{\partial f_i}{\partial x_j}(\mathbf{x}) \right)^2} \right\}_{j=1}^n \right)$

i.e., it holds for every quadratically inner-bounded functions, but *not* sufficient.

In addition to this, our recent work [27] also pinpoints some mistakes in the numerical section of [6], [28], where we provide the corresponding correct conditions. The next section focuses on the development of an interval-based algorithm to solve global maximization problems.

IV. INTERVAL-BASED GLOBAL MAXIMIZATION

After showing that the parameterization of NDS can actually be transformed into solving global maximization problems, our next step is finding a way to solve such problems. In general there are two distinct approaches that can be pursued in solving global optimization problems: *point-based method* and *interval-based method* [37]. Note that the disadvantages of the former include the lack of optimality guarantees and the possibility of such methods converging to local maxima/minima [37]. In the context of NDS parameterization, if the solution from point-based optimization algorithms is suboptimal, then the resulting parameter is an *inner approximation*. For the interval-based algorithm, however, as it provides both upper and lower bounds towards the optimal solution, we can use the upper bound to compute the corresponding parameter of the NDS. Considering this point, in this paper we utilize an interval-based global optimization method for NDS parameterization. In the sequel, we discuss this approach in a detailed manner, starting from the concept of interval arithmetic and interval function.

A. Fundamentals of Interval Arithmetic and Interval Function

The most important building block in interval arithmetic (IA) is, rather unsurprisingly, an interval itself. An interval is a closed

nonempty subset of \mathbb{R} characterized by its upper and lower bounds. That is, an interval $[a, b]$ over the reals is defined as

$$[a, b] := \{x \in \mathbb{R} \mid a \leq x \leq b\}.$$

In IA, it is common to represent a real variable x by its interval so that $x \in [x] := [\underline{x}, \bar{x}]$. It follows directly from its definition that $\underline{x} = \inf([x])$ and $\bar{x} = \sup([x])$. An interval $[x]$ is said to be *degenerate* if it only contains one element x such that $x = \underline{x} = \bar{x}$. It is obvious that an interval $[x]$ is positive (nonnegative) if $\underline{x} > 0$ ($\underline{x} \geq 0$) and negative (nonpositive) if $\bar{x} < 0$ ($\bar{x} \leq 0$). Two intervals $[x]$ and $[y]$ are considered *equal* when $\underline{x} = \underline{y}$ and $\bar{x} = \bar{y}$. A partial ordering of intervals is defined as follow: $[x] < [y]$ if and only if $\bar{x} < \underline{y}$. The midpoint (or center) and width of an interval $[x]$ are respectively defined as

$$\text{mid}([x]) := \frac{1}{2}(\underline{x} + \bar{x}), \quad \text{width}([x]) := \bar{x} - \underline{x}.$$

For brevity, we define $||x|| := \text{width}([x])$. A binary operation of two intervals $X := [x]$ and $Y := [y]$ is defined as follow

$$X \diamond Y := \{z \in \mathbb{R} \mid z = x \diamond y, x \in X, y \in Y\},$$

where the notation \diamond represents any binary operator from the set of elementary arithmetic operators $\{+, -, \times, \div\}$. Readers are referred to [25], [38] for more comprehensive IA operations.

An n -orthotope $\mathcal{S} = \prod_{i \in \mathbb{I}(n)} \mathcal{S}_i$ can be regarded as an *element* of n -dimensional intervals \mathbb{IR}^n , i.e., $\mathcal{S} \in \mathbb{IR}^n$ and consequently $\mathcal{S}_i \in \mathbb{IR}$. By definition, the notion $z \in \mathcal{S}$ means that $z_i \in \mathcal{S}_i$ for all $i \in \mathbb{I}(n)$. For two n -orthotopes $\mathcal{S}, \mathcal{S}' \in \mathbb{IR}^n$, the notion $\mathcal{S} \subseteq \mathcal{S}'$ holds if for all $i \in \mathbb{I}(n)$ we have $\mathcal{S}_i \subseteq \mathcal{S}'_i$ [39]. The interval representation of a real-valued function $f(\cdot)$ is denoted by $f^I(\cdot)$ [40]. Such function is generally referred to as *interval-valued function*. An interval function $f^I(\cdot)$, which is an interval representation of $f(\cdot)$, is termed as an *interval extension* of $f(\cdot)$ —see Definition 1.

Definition 1. Let $f : \mathbb{R}^n \rightarrow \mathbb{R}$ be a mapping with $\mathcal{S} \subset \mathbb{R}^n$ as the domain of interest. An interval function $f^I : \mathbb{IR}^n \rightarrow \mathbb{IR}$ is said to be an *interval extension* of $f(\cdot)$ if, for all $z \in \mathcal{S}$, $f(z) = f^I([z, z])$ where $[z, z] = \prod_{i \in \mathbb{I}(n)} [z_i, z_i]$.

The construction of $f^I(\cdot)$ can be done by simply substituting each occurrence of x_i in $f(\cdot)$ with \mathcal{S}_i for all $i \in \mathbb{I}(n)$ [37]. At this point, we should be aware of one particular disadvantage of IA referred to as *dependency effect*: the interval evaluation of $f(\cdot)$ depends on the expression of $f(\cdot)$ used to implement the computation [37]. The following example demonstrates the dependency effect in IA.

Example 2. Consider the function $f(x) = x^3 - 1$ defined on the interval $[x] = [-2, 3]$. The interval evaluation of $f(\cdot)$ in this particular domain for two different expressions are

$$[x]^3 - 1 = [-9, 26] \quad (25a)$$

$$([x] - 1)([x]^2 + [x] + 1) = [-39, 26]. \quad (25b)$$

It is seen that albeit (25a) and (25b) represent the same function, the corresponding interval evaluations yield different values.

With that in mind, in using IA for solving global optimization problems, one has to carefully choose the way of expressing the interval extension of the objective value in order to obtain the best results. Readers are referred to [41] for methods and tricks on expressing interval functions that could give tighter

bounds. The next definition presents one important property of an interval extension, namely *inclusion isotonic*, which is very useful for computing interval extensions.

Definition 2. Let $f : \mathbb{R}^n \rightarrow \mathbb{R}$ be a mapping with $f^I : \mathbb{IR}^n \rightarrow \mathbb{IR}$ as its interval extension. For $\mathcal{S}, \mathcal{S}' \in \mathbb{IR}^n$ such that $\mathcal{S}_i \subseteq \mathcal{S}'_i$ for every $i \in \mathbb{I}(n)$, then $f^I(\cdot)$ is *inclusion isotonic* if and only if $f^I(\mathcal{S}) \subseteq f^I(\mathcal{S}')$.

In practical implementation and computation of IA, which is usually performed using computer programs/software having finite-precision floating point representation, it is only possible to compute the rounding of interval extension of a function $f(\cdot)$. Due to this reason, in this paper we assume that computer programs represent real numbers using outward rounding [42]. This assumption produces a useful attribute: every interval extension of any real function satisfies the inclusion isotonic property [40]. The fundamental theorem of interval arithmetic, presented below, guarantees that any interval extension of a real function satisfying the inclusion isotonicity encompasses the range of that function [40]. This has become the most important result in interval analysis.

Lemma 3 (Fundamental Theorem of Interval Arithmetic). Let $f^I : \mathbb{IR}^n \rightarrow \mathbb{IR}$ be an interval extension of $f : \mathbb{R}^n \rightarrow \mathbb{R}$ which is inclusion isotonic. Then, for all $z_i \in \mathcal{S}_i$ where $i \in \mathbb{I}(n)$ and $\mathcal{S} \in \mathbb{IR}^n$, $f^I(\mathcal{S})$ contains the range of $f(z)$.

The proof of Lemma 3 can be obtained from [40]. In the above lemma, the range of $f(\cdot)$ for a given domain \mathcal{S} is defined as $\text{range}(f) := [\inf_{z \in \mathcal{S}} f(z), \sup_{z \in \mathcal{S}} f(z)]$. If we know the domain of $f(\cdot)$, then we simply refer the upper and lower bounds of the range of $f(\cdot)$ as $\sup f(z)$ and $\inf f(z)$ —the same goes for expressing the upper and lower bounds of any interval-valued function. For the sake of simplicity, we write $f(\mathcal{S})$ to represent the range of $f(\cdot)$, that is, $f(\mathcal{S}) = \text{range}(f)$. The fundamental theorem of arithmetic ensures that $f(\mathcal{S}) \subseteq f^I(\mathcal{S})$ always holds for any valid $f^I(\cdot)$. Nonetheless, to obtain the best possible result, we prefer to consider $f^I(\cdot)$ with endpoints that are close to those of $f(\cdot)$, since such $f^I(\cdot)$ contains the best information regarding the range of the image of $f(\cdot)$. An interval extension $f^I(\cdot)$ satisfying $f^I(\mathcal{S}) = f(\mathcal{S})$ is said to be *minimal* or *exact*, and we say that its endpoints are *sharp* [37], [40]. Next, we discuss the principle of solving global maximization problems based on IA.

B. Global Maximization Using Interval Arithmetic

We start this section by considering the following problem

$$h := \max_{\omega \in \Omega} h(\omega), \quad (26)$$

where the function $h : \mathbb{R}^p \rightarrow \mathbb{R}$ denotes the objective function to be maximized inside a p -orthotope Ω and h denotes the objective function value. Since we do not have any constraint other than Ω , then Problem (26) is categorized as *unconstrained global maximization problem*. The above problem generalizes the way of computing the corresponding constants for each class of nonlinearity presented in Tab. 1. In the sequel we adopt the following conventions: the notion ω^* denotes any maximizer of problem (26) and $h^* = h(\omega^*)$ denotes the optimal value of (26). For this problem to be meaningful, it is assumed throughout this section that $\omega^* \in \Omega$.

Algorithm 1: Interval-Based Algorithm for Unconstrained Global Maximization

```

1 input:  $\Omega$ ,  $\epsilon_h$ ,  $\epsilon_\Omega$ ,  $h(\cdot)$ ,  $h^I(\cdot)$ 
2 initialize:  $\mathcal{S}_1 = \Omega$ ,  $C = \{\mathcal{S}_1\}$ ,  $\tilde{C} = \emptyset$ 
3 compute:  $\bar{\mathcal{S}} = \arg \max_{\mathcal{S}_i \in C} \sup(h^I(\mathcal{S}_i))$ ,
    $u = \sup(h^I(\bar{\mathcal{S}}))$ ,  $l = h(\text{mid}(\mathcal{S}_1))$ 
4 while  $u - l > \epsilon_h$  and  $|\bar{\mathcal{S}}| > \epsilon_\Omega$  do
5    $\{C, \bar{\mathcal{S}}, l, u\} \leftarrow \text{OptBnB}(C, \bar{\mathcal{S}}, l)$ 
6 if  $u - l > \epsilon_h$  then
7   foreach  $\mathcal{S}_j \in C$  and  $|\mathcal{S}_j| > \epsilon_\Omega$  do
8      $\tilde{C} \leftarrow \tilde{C} \cup \{\mathcal{S}_j\}$ 
9 while  $u - l > \epsilon_h$  and  $\tilde{C} \neq \emptyset$  do
10    $\bar{\mathcal{S}} \leftarrow \arg \max_{\mathcal{S}_i \in \tilde{C}} \inf(h^I(\mathcal{S}_i))$ 
11    $\{C, \bar{\mathcal{S}}, l, u\} \leftarrow \text{OptBnB}(C, \bar{\mathcal{S}}, l)$ ,  $\tilde{C} \leftarrow \emptyset$ 
12   foreach  $\mathcal{S}_j \in C$  and  $|\mathcal{S}_j| > \epsilon_\Omega$  do
13      $\tilde{C} \leftarrow \tilde{C} \cup \{\mathcal{S}_j\}$ 
14 if  $u - l > \epsilon_h$  then
15   foreach  $\mathcal{S}_j \in C$  do
16      $l \leftarrow \max(l, h(\inf(\mathcal{S}_j)), h(\sup(\mathcal{S}_j)))$ 
17     foreach  $\mathcal{S}_k \in C$  do
18       if  $\sup(h^I(\mathcal{S}_k)) < l$  then
19          $C \leftarrow C \setminus \{\mathcal{S}_k\}$ 
20       if  $u - l \leq \epsilon_h$  then
21         break
22 output:  $C, l, u$ 

```

The term *interval-based algorithm* is used in this paper to refer any algorithm that utilizes IA for solving global optimization problem. IA has been widely utilized over past decades for solving global optimization problems, either constrained or unconstrained—see the work in [37], [40]–[42]. The purpose of our interval-based algorithm is to search for the best interval containing h^* . Interval-based algorithm belongs to a larger group of algorithms classified as *branch and bound* (BnB) algorithm [37]. In the simplest way, the working principles of BnB algorithm can be categorized into *branching* and *bounding*. In the branching step, Problem (26) is divided into smaller subproblems, which is carried out by dividing the set Ω into several smaller subsets. We then compute the bounds for each subproblems and remove the corresponding subsets that do not contain any maximizer. This step is referred to as the bounding step. These two steps are performed iteratively until the best solution is obtained. In what follows we present some important definitions and theorems that have become the essence of the algorithm. The following definition describes the concept of *cover* for sets [43].

Definition 3. Let Ω be a set. If $C = \{\mathcal{S}_i\}_{i=1}^N$ is a sequence of N nonempty subsets of Ω , then we say that C is a *cover* in Ω . Specifically, if the following holds

$$\Omega = \bigcup_{i \in \mathbb{I}(N)} \mathcal{S}_i,$$

then we say that C is a *cover* for Ω .

Algorithm 2: *OptBnB*

```

1 input:  $C, \mathcal{S}', l$ 
2  $C \leftarrow C \setminus \{\mathcal{S}'\}$ ,  $\Omega' = \arg \max_{\Omega_i \in \mathcal{S}'} |\Omega_i|$ 
3  $\Omega'_l = [\inf(\Omega'), |\Omega'|]$ ,  $\Omega'_r = [|\Omega'|, \sup(\Omega')]$ 
4  $\mathcal{S}_l = \Omega'_1 \times \cdots \times \Omega'_l \times \cdots \times \Omega'_p$ ,
    $\mathcal{S}_r = \Omega'_1 \times \cdots \times \Omega'_r \times \cdots \times \Omega'_p$ 
5  $C \leftarrow C \cup \{\mathcal{S}_l, \mathcal{S}_r\}$ 
6  $\mathcal{S}_m = \arg \max_{\mathcal{S}_i \in C} \inf(h^I(\mathcal{S}_i))$ 
7  $l \leftarrow \max(l, h(\text{mid}(\mathcal{S}_m)))$ 
8 foreach  $\mathcal{S}_i \in C$  do
9   if  $\sup(h^I(\mathcal{S}_i)) < l$  then
10     $C \leftarrow C \setminus \{\mathcal{S}_i\}$ 
11  $\mathcal{S}'' = \arg \max_{\mathcal{S}_i \in C} \sup(h^I(\mathcal{S}_i))$ ,  $u = \sup(h^I(\mathcal{S}''))$ 
12 output:  $C, \mathcal{S}'', l, u$ 

```

In the above definition, $N := \text{card}(C)$, which denotes the number of elements in C . The following proposition provides the bounds for the optimal solution of problem (26) given that a cover C in Ω contains a maximizer—a principle that has become paramount for the interval-based algorithm.

Proposition 4. Let ω^* be a maximizer for problem (26). If $C = \{\mathcal{S}_i\}_{i=1}^N$ is a cover in Ω that contains a maximizer, then we have $h^* \in [l, u]$ where

$$l = \max_{\mathcal{S}_i \in C} \inf(h^I(\mathcal{S}_i)), \quad u = \max_{\mathcal{S}_i \in C} \sup(h^I(\mathcal{S}_i)). \quad (27)$$

Proof. Suppose that the cover $C = \{\mathcal{S}_i\}_{i=1}^N$ in Ω contains a maximizer for problem (26). As C contains a maximizer, then $\omega^* \in \mathcal{S}_j$ for some $j \in \mathbb{I}(N)$, which in turn implies that $h^* \leq \sup(h^I(\mathcal{S}_j))$. Since $\sup(h^I(\mathcal{S}_j)) \leq u$, then it follows that $h^* \leq u$. Next, consider $\mathcal{S}_k \in C$ such that $l = \inf(h^I(\mathcal{S}_k))$. As $\mathcal{S}_k \neq \emptyset$, then there exists some points $\omega \in \mathcal{S}_k$ for which $h(\omega) \leq h^*$. However, since $\inf(h^I(\mathcal{S}_k)) \leq h(\omega)$, then $l \leq h^*$. This shows that $l \leq h^* \leq u$. ■

The minimization version of Proposition 4 was proposed in [43], which in this paper, is modified and presented accordingly for maximization problem as we attempt to solve (26). In every iteration of this interval-based algorithm, the branching step produces a sequence of subsets of Ω in such a way that it forms a cover C containing a maximizer. In the bounding step, we then remove all subsets in the cover that positively do not contain any maximizer. The following proposition states that any subset $\mathcal{S} \in C$ that satisfy $\sup(h^I(\mathcal{S})) < l$ where l is defined in (27) does not contain any maximizer. Therefore, such subset may be removed from C .

Proposition 5. Let ω^* be a maximizer for problem (26) and $C = \{\mathcal{S}_i\}_{i=1}^N$ be a cover in Ω containing a maximizer. If there exists $\mathcal{S}_j \in C$ for some $j \in \mathbb{I}(N)$ such that $\sup(h^I(\mathcal{S}_j)) < l$, then $\omega^* \notin \mathcal{S}_j$.

Proof. Note that, as the cover C contains a maximizer, then from Proposition 4 it holds that $l \leq h^* \leq u$. By contradiction, suppose that there exists such $\mathcal{S}_j \in C$, where $j \in \mathbb{I}(N)$, that $\sup(h^I(\mathcal{S}_j)) < l$ and $\omega^* \in \mathcal{S}_j$. However, since the assertion $\omega^* \in \mathcal{S}_j$ implies $h^* \leq \sup(h^I(\mathcal{S}_j))$, we must have $h^* < l$, which is a contradiction. ■

Having discussed the basic principles of interval-based algorithm, in the next section a more detailed way of constructing an actual interval-based algorithm to solve (26) is presented.

C. Interval-Based Algorithm by BnB Routines

The objective of the interval-based algorithm is to find the best (*smallest*) interval $[l, u]$ containing h^* . If this interval is degenerate, then we have successfully found h^* . Otherwise in the case when $l < u$, we are assured that the optimal solution cannot be greater than u and smaller than l . This can be achieved by iteratively decreasing the upper bound u and increasing the lower bound l . The reduction of u can be performed by splitting a subset $\mathcal{S} \in C$ having the biggest upper bound of interval evaluation in C . Likewise, increasing l can be done by splitting subset $\mathcal{S} \in C$ having the smallest lower bound in C . To that end, we present an interval-based algorithm—given in Algorithm 1—for solving problem (26). In this algorithm, it is necessary to define two positive constants ϵ_h and ϵ_Ω : the constant ϵ_h is useful to bound the interval containing the optimal solution, whereas ϵ_Ω is useful to provide a lower bound towards the width of all subsets \mathcal{S}_i in the cover—if the width of a subset \mathcal{S}_i is smaller than ϵ_Ω , then we assume that \mathcal{S}_i cannot be split into two smaller subsets. The *width* of a subset \mathcal{S}_i is defined as

$$|\mathcal{S}_i| := \max_{\Omega_j \in \mathcal{S}_i} |\Omega_j|.$$

The algorithm is said to be successful in computing the best solution when it holds that $u - l \leq \epsilon_h$ —in this case, we say that h^* is ϵ_h -optimal. Otherwise, $u - l$ is the smallest interval containing h^* that can be obtained. As such, either l or u cannot be further improved because the widths of every $\mathcal{S}_i \in C$ are all less than ϵ_Ω , thus they cannot be split to produce even smaller subsets (we refer to such subset as *atomic* [37]).

It is important to note that this algorithm is a modification of Algorithm MS3 proposed in [37] with two main differences. Firstly, Algorithm 1 is specifically designed for solving global maximization problem (26) and presented using rigorous mathematical notations for the ease of analysis and implementation, and secondly, we have added an *explicit* additional step to ensure that the splitting of a subset $\mathcal{S} \in C$ is possible only when the width of \mathcal{S} is greater than ϵ_Ω . In what follows, we show that Algorithm 1 computes the best interval for h^* .

Theorem 7. *When Algorithm 1 terminates, then*

- 1) $h^* \in [l, u]$, where $[l, u]$ is the best interval for h^* ,
- 2) $\omega^* \in C = \prod_{i \in \mathbb{I}(N)} \mathcal{S}_i$ where C is a cover in Ω at the end of the algorithm.

Proof. We start by assuming that Ω is nonempty such that $\omega^* \in \Omega$. From the initialization, obviously C contains the maximizer. In the first part, we will show that the first loop in Step 4 computes the best upper bound for h^* . Note that, due to Proposition 4, at every instance we always have $l \leq h^* \leq u$ with $\omega^* \in C$. Since $u = \sup(h^I(\mathcal{S}))$ where \mathcal{S} is an element of C with the greatest upper bound, it is divided into two subsets namely \mathcal{S}_l and \mathcal{S}_r . As $\mathcal{S}_l \subset \mathcal{S}$ and $\mathcal{S}_r \subset \mathcal{S}$, by inclusion isotonicity, it then holds that $h^I(\mathcal{S}_l) \subset h^I(\mathcal{S})$ and $h^I(\mathcal{S}_r) \subset h^I(\mathcal{S})$, implying that $\sup(h^I(\mathcal{S}_l)) < \sup(h^I(\mathcal{S}))$ and $\sup(h^I(\mathcal{S}_r)) < \sup(h^I(\mathcal{S}))$. This shows that splitting of \mathcal{S} yields a better upper bound. In Algorithm 2, any $\mathcal{S}_i \in C$

Algorithm 3: Computing Lipschitz Constant γ_{l_1} or γ_{l_2}

```

1 input:  $\Omega, \epsilon_h, \epsilon_\Omega, f(\cdot)$ 
2 switch  $\gamma_l$  do
3   case  $\gamma_{l_1}$  do
4     define:  $h(x, u) := \sum_{i \in \mathbb{I}(g)} \|\nabla_x f_i(x, u)\|_2^2$  and
       construct  $h^I(x, u)$ 
5     obtain:  $u$  from Algorithm 1 given  $\Omega, \epsilon_h, \epsilon_\Omega, h(\cdot), h^I(\cdot)$ 
6     output:  $\gamma_{l_1} = \sqrt{u}$ 
7   case  $\gamma_{l_2}$  do
8     foreach  $i \in \mathbb{I}(g)$  do
9       define:  $h_i(x, u) := \|\nabla_x f_i(x, u)\|_2^2$  and
         construct  $h_i^I(x, u)$ 
10      obtain:  $u_i$  from Algorithm 1 given  $\Omega, \epsilon_h, \epsilon_\Omega, h_i(\cdot), h_i^I(\cdot)$ 
11      output:  $\gamma_{l_2} = \sqrt{\sum_{i \in \mathbb{I}(g)} u_i}$ 

```

satisfying $\sup(h^I(\mathcal{S}_i)) < l$ may be discarded since, according to Proposition 5, such subset does not contain any maximizer. Thus, we always have $\omega^* \in C$ and $l \leq h^* \leq u$. When the first loop in Step 4 terminates, we have $u - l \leq \epsilon_h$ —therefore, h^* is ϵ_h -optimal and the algorithm terminates—or $u - l > \epsilon_h$. In the latter, $|\bar{\mathcal{S}}| \leq \epsilon_\Omega$ hence it cannot be split further. Either case, we have u as the best upper bound for h^* .

In the second part, it will be shown that l provides the best lower bound for h^* . Keep in mind that the temporary cover \tilde{C} may be nonempty only if $u - l > \epsilon_h$ and there exists $\mathcal{S}_i \in C$ such that $|\mathcal{S}_i| > \epsilon_\Omega$. Note that $\bar{\mathcal{S}} \notin \tilde{C}$. Since we split $\bar{\mathcal{S}}$ into two subsets namely \mathcal{S}_l and \mathcal{S}_r where $\bar{\mathcal{S}}$ is an element of \tilde{C} with the biggest lower bound, then as demonstrated above, we have $h^I(\mathcal{S}_l) \subset h^I(\bar{\mathcal{S}})$ and $h^I(\mathcal{S}_r) \subset h^I(\bar{\mathcal{S}})$, implying that $\inf(h^I(\bar{\mathcal{S}})) < \inf(h^I(\mathcal{S}_l))$ and $\inf(h^I(\bar{\mathcal{S}})) < \inf(h^I(\mathcal{S}_r))$. This shows that we attain a better lower bound by splitting $\bar{\mathcal{S}}$. When the second loop in Step 9 terminates, we have obtained a ϵ_h -optimal solution or every $\mathcal{S}_i \in C$ satisfies $|\mathcal{S}_i| \leq \epsilon_\Omega$ —thus $\tilde{C} = \emptyset$. At this point, every subsets in C cannot be split further. Thus, when $u - l > \epsilon_h$, l can be updated by evaluating objective function evaluation of corner points on each $\mathcal{S}_i \in C$ and removing $\mathcal{S}_j \in C$ satisfying $\sup(h^I(\mathcal{S}_j)) < l$. At the end of Algorithm 1, we have achieved $u - l \leq \epsilon_h$ or $u - l > \epsilon_h$ —in the former case, we have a ϵ_h -optimal solution. Either case, $[l, u]$ is the best interval containing h^* . Since we know that $\omega^* \in C$, there exists \mathcal{S}_j for some $j \in \mathbb{I}(N)$ for which $\omega^* \in \mathcal{S}_j$. Thus, it immediately follows that $\omega^* \in \prod_{i \in \mathbb{I}(N)} \mathcal{S}_i$. This ends the proof. ■

After Algorithm 1 terminates, we use u —the upper bound—to compute the corresponding constants for function sets listed in Tab. I—see Section IV-D. As the lower bound l is not required to compute these constants, basically one can stop Algorithm 1 when the first loop in Step 4 terminates. However, by obtaining the best lower bound l , it gives us a sense on the location of h^* as well as an optimality certificate through the definition of ϵ_h -optimal.

Remark 3. *The lower bound l in Algorithm 1 is determined via the evaluation of objective function based on the midpoint of*

the corresponding subset, say, \mathcal{S}_i . As discussed in [37], one can also use the evaluation of either side of the corners of \mathcal{S}_i . Other than these simple approaches, one can also use a more complicated deterministic point-based technique, such as gradient ascent, Newton method, conjugate gradient method, and interior-point method, as well as stochastic ones such as quasi random algorithms and heuristics. This way, more subsets can potentially be removed from C , albeit it is likely that the computational time will increase.

D. How One Should Use Such Interval-Based Algorithm for NDS Parameterization?

The parameterization of nonlinear function $f(\cdot)$ of NDS (2) using the proposed interval-based algorithm is now discussed. In the prior section, a methodology to compute the best bounds for the optimal solution of a general unconstrained maximization problem described in (26) is thoroughly presented—see Algorithm 1. Note that this algorithm essentially paves the way for NDS parameterization, i.e., computing the corresponding parameters for bounded Jacobian, Lipschitz continuous, one-sided Lipschitz, quadratically inner-bounded, and quadratically bounded function sets. For the sake of brevity, in what follows we show how Algorithm 1 can be employed for NDS parameterization specifically for Lipschitz continuous function set.

First recall that in Section III-B we described two methods for computing Lipschitz constant: γ_{l_1} as given in (7b) and γ_{l_2} as given in (8). To obtain these constants using the proposed interval-based algorithm, first it is necessary to define functions $h : \mathbb{R}^n \times \mathbb{R}^m \rightarrow \mathbb{R}$ and $h^I : \mathbb{IR}^n \times \mathbb{IR}^m \rightarrow \mathbb{IR}$, where $h(\cdot)$ is the objective function to be maximized while $h^I(\cdot)$ is the corresponding interval expression of $h(\cdot)$. Note that $h(\cdot)$ is constructed from (7b) and (8). Since the expression $h^I(\cdot)$ determines the resulting interval, it is crucial to express $h^I(\cdot)$ in such a way that $h^I(\cdot)$ is as close as possible to the exact/minimal formulation of interval extension of $h(\cdot)$. This could allow us to reduce/minimize the dependency effect in our algorithm. Upon choosing the region of interest Ω and the values for ϵ_h and ϵ_Ω , Lipschitz constant γ_l can be determined as either γ_{l_1} or γ_{l_2} . This process is summarized in Algorithm 3. The computation of bounded Jacobian, one-sided Lipschitz, quadratically inner-bounded, and quadratically bounded constants can be carried out using similar steps—the details to parameterize NDS for other type of function set is omitted here due to space constraint.

We now discuss important remarks and strategies related to the computational performance of the IA-based algorithm for NDS parameterization.

- The first strategy is referred to as search space reduction, as mentioned in Remark 1. In the context of Lipschitz parameterization, there is a possibility that not every components of \mathbf{x} and \mathbf{u} appears as an argument in $\nabla_x f_i(\mathbf{x}, \mathbf{u})$. Thus it makes sense to ignore these components from Ω such that we only need to solve $\max_{(\mathbf{x}, \mathbf{u}) \in \Omega_{r_i}} \|\nabla_x f_i(\mathbf{x}, \mathbf{u})\|_2^2$ where Ω_{r_i} denotes the reduced search space.
- The second strategy exploits the structure of $f(\cdot)$. Some real world dynamic systems such as water, energy, traffic, and combustion networks are comprised of many individual subsystems that are intertwined together, forming a

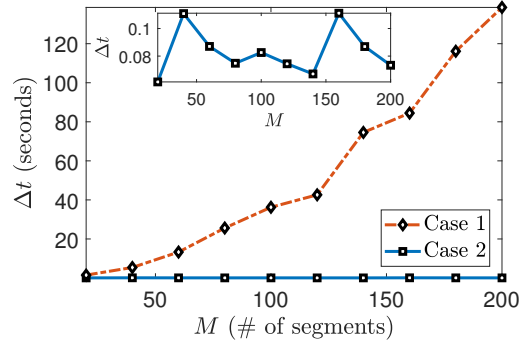


Figure 2. Comparison between computational time (Δt) for computing Lipschitz constants and the number of segments on the main highway.

complex networked NDS. The majority of these subsystems may have similar nonlinear dynamics defined on the same set. As an illustration, let $f_i(\cdot)$ and $f_j(\cdot)$ be the corresponding nonlinearities of subsystems i and j with similar domain Ω_i and Ω_j . When $f_i(\cdot)$ and $f_j(\cdot)$ are comprised of the same structure, one only need to solve $\max_{(\mathbf{x}, \mathbf{u}) \in \Omega_i} \|\nabla_x f_i(\mathbf{x}, \mathbf{u})\|_2^2$ when computing Lipschitz constant because, as $f_j(\cdot)$ is similar to $f_i(\cdot)$, the optimal value of this problem is valid for both i and j .

- In the third strategy, the computation of Lipschitz constant is performed in a distributive fashion. By doing so, the computational burden to compute Lipschitz constant is distributed as the problem $\max_{(\mathbf{x}, \mathbf{u}) \in \Omega} \|\nabla_x f_i(\mathbf{x}, \mathbf{u})\|_2^2$ is solved in parallel for each $i \in \mathbb{I}(g)$, therefore reducing the overall computational time.

The second strategy implies that the complexity of the proposed approach does not necessarily depend on the problem dimension. Instead, it depends on the number of different nonlinearities in the NDS. At last, it is always possible to combine these strategies altogether to get even less complexity. The next section demonstrates the effectiveness and scalability of the proposed approach to parameterize NDS with different function sets.

V. NUMERICAL EXAMPLES

In this section we showcase the proposed methodologies and algorithms for parameterizing some NDS that include traffic networks, synchronous generator, and the motion of a moving object into the following function sets: Lipschitz continuous, one-sided Lipschitz, and quadratically inner-bounded. All simulations are performed using MATLAB R2017b running on a 64-bit Windows 10 with 2.5GHz Intel[®] Core[™] i7-6500U CPU and 16 GB of RAM. YALMIP's [44] optimization package together with MOSEK's [45] SDP solver are used to solve any semidefinite programs.

A. Lipschitz Parameterization for Traffic Networks

The dynamic model of traffic networks, particularly on a stretched highway consisting inflow and outflow ramps, can be modeled by partitioning it into several segments of equal length l such that the dynamics of each highway segment can be expressed in the form of ordinary differential equations [46]

$$\dot{\rho}_i(t) = \frac{1}{l} \left(\sum q_{i-1}(t) - \sum q_i(t) \right),$$

where q_{i-1} and q_i represent any inflow and outflow ramps, and ρ_i represents traffic density on that segment. The above model

Table III

NUMERICAL TEST RESULTS FOR LIPSCHITZ CONSTANTS COMPUTATION ON TRAFFIC NETWORKS. NOTATIONS: $\#split$ INDICATES HOW MANY SPLITTING PROCESSES ARE PERFORMED, $\#subset$ DENOTES THE NUMBER OF SUBSETS IN THE LAST COVER C , gap REFERS TO OPTIMALITY GAP, WHICH ESSENTIALLY COMPUTES THE DIFFERENCE BETWEEN u AND l , AND $\epsilon_h-opt?$ IS CHECKED WHEN THE SOLUTION IS ϵ_h -OPTIMAL.

M	Case 1						Case 2					
	γ_{l_1}	Δt (s)	$\#split$	$\#subset$	$gap (\times 10^{-5})$	$\epsilon_h-opt?$	γ_{l_2}	Δt (s)	$\#split$	$\#subset$	$gap (\times 10^{-5})$	$\epsilon_h-opt?$
20	0.4033	1.49	236	86	9.757	✓	0.4033	0.061	83	16	7.62	✓
40	0.5651	5.40	492	202	9.853	✓	0.5651	0.110	83	16	7.62	✓
60	0.6900	13.29	761	331	9.997	✓	0.6900	0.087	83	16	7.62	✓
80	0.7955	25.61	1041	471	9.997	✓	0.7955	0.075	83	16	7.62	✓
100	0.8886	36.24	1321	611	9.997	✓	0.8886	0.083	83	16	7.62	✓
120	0.9728	42.60	1619	769	9.974	✓	0.9728	0.074	83	16	7.62	✓
140	1.0503	74.56	1919	929	9.974	✓	1.0503	0.067	83	16	7.62	✓
160	1.1224	84.46	2219	1089	9.974	✓	1.1224	0.110	83	16	7.62	✓
180	1.1902	116.1	2519	1249	9.974	✓	1.1902	0.087	83	16	7.62	✓
200	1.2543	138.6	2819	1409	9.974	✓	1.2543	0.073	83	16	7.62	✓

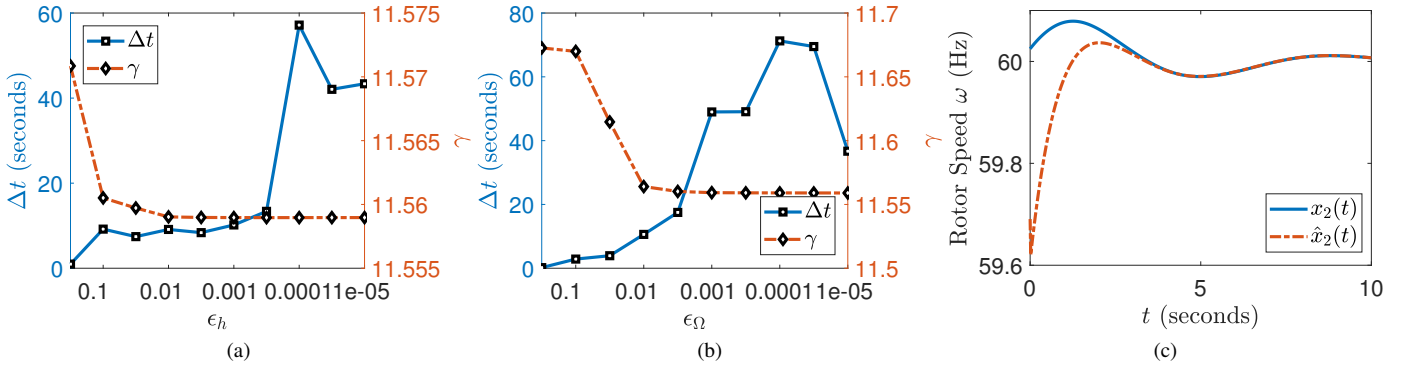


Figure 3. Numerical test results for synchronous generator: (a) computational time (Δt) and Lipschitz constant (γ) for various ϵ_h , (b) the corresponding results for various ϵ_Ω , and (c) the trajectories of estimated and actual generator rotor speed (ω) using a Lipschitz-based observer [1] with $\gamma = 11.559$.

assumes that the highway is uncongested—in this situation, the traffic density satisfies $\rho_i \in [0, \rho_c]$ where ρ_c denotes the critical density. By employing Greenshield's fundamental diagram to represent the relation between traffic density and traffic flow [47], the nonlinearity of the overall dynamic model for this particular system (supposing that no segment is connected to both inflow and outflow ramps) can be distinguished into five different types of nonlinearities, detailed as follows [46], [48]

$$a) f_a(\mathbf{x}) = \delta x_i^2 \quad (28a)$$

$$b) f_b(\mathbf{x}) = \delta (x_i^2 - x_{i-1}^2 - x_j^2) \quad (28b)$$

$$c) f_c(\mathbf{x}) = \delta (x_i^2 - x_{i-1}^2) \quad (28c)$$

$$d) f_d(\mathbf{x}) = \delta (x_i^2 - x_{i-1}^2 + \alpha_j x_j^2) \quad (28d)$$

$$e) f_e(\mathbf{x}) = -\delta \alpha_i x_i^2, \quad (28e)$$

where $x_i := \rho_i$ and $\delta := \frac{v_f}{l\rho_m}$; v_f and ρ_m denote the free flow speed and maximum density (maximum density ρ_m is equal to $2\rho_c$). In this case, the following values, which are adapted from [49], are considered: $v_f = 31.3$ m/s, $\rho_m = 0.053$ vehicles/m, and $l = 500$ m. The splitting ratio for outflow ramp is chosen to be $\alpha_i = \alpha_j = 0.5$. The main stretched highway is divided into M segments where the 2^{nd} is connected to an inflow ramp and the $(M-1)^{\text{th}}$ is connected to an outflow ramp such that there are $M+2$ number of segments in total, which means that the total number of states is $n = M+2$. The region of interest is set to be $\Omega = [0, \rho_c]^n$ since the traffic is uncongested.

In this numerical test we consider two cases: the first cases utilizes (7b) while the second one utilizes (8) for computing Lipschitz constants. Specifically in Case 2, the corresponding set Ω

is reduced so that the variables considered in the computation of $\max_{\mathbf{x} \in \Omega} \|\nabla_x f_z(\mathbf{x})\|_2^2$ for each $z \in \{a, b, c, d, e\}$ in (28) are only the ones that appear in the expression of (28), as discussed in Remark 1. For clarity, the expressions of $\|\nabla_x f_z(\mathbf{x})\|_2^2$ for each z are listed as follows

$$a) \|\nabla_x f_a(\mathbf{x})\|_2^2 = 4\delta^2 x_i^2 \quad (29a)$$

$$b) \|\nabla_x f_b(\mathbf{x})\|_2^2 = 4\delta^2 (x_i^2 + x_{i-1}^2 + x_j^2) \quad (29b)$$

$$c) \|\nabla_x f_c(\mathbf{x})\|_2^2 = 4\delta^2 (x_i^2 + x_{i-1}^2) \quad (29c)$$

$$d) \|\nabla_x f_d(\mathbf{x})\|_2^2 = 4\delta^2 (x_i^2 + x_{i-1}^2 + \alpha_j^2 x_j^2) \quad (29d)$$

$$e) \|\nabla_x f_e(\mathbf{x})\|_2^2 = 4\delta^2 \alpha_i^2 x_i^2. \quad (29e)$$

In this test we compare different values of segments such that $M = 20, 40, \dots, 200$. Since it is only M that changes and all segments in the main highway (from $i = 3$ to $i = M-2$) have the same nonlinearity—represented by (28c)—then by applying the second strategy discussed in Section IV-D, it is sufficient to solve $\max_{\mathbf{x} \in \Omega} \|\nabla_x f_c(\mathbf{x})\|_2^2$ once. Constants ϵ_h and ϵ_Ω for Algorithm 1 are set to be 1×10^{-4} and 1×10^{-7} respectively. The interval expressions for (29) are constructed based on interval arithmetic rules described in [25], [40], [42].

After running Algorithm 3 using the aforementioned settings, we obtain results that are detailed in Tab. III. All of the computed Lipschitz constants γ_{l_1} and γ_{l_2} are ϵ_h -optimal, since the gap between u and l are all less than the predefined ϵ_h . Interestingly, notice that the values of γ_{l_1} and γ_{l_2} are the same for both forms. This demonstrates that the formulations posed in (7b) and (8) can indeed compute the same solutions for some cases. From Fig. 2, we see that the computation of Lipschitz

Table IV
NUMERICAL TEST RESULTS FOR LIPSCHITZ CONSTANTS COMPUTATION ON SYNCHRONOUS GENERATOR.

ϵ_Ω or ϵ_h	$\epsilon_h = 1 \times 10^{-5}$						$\epsilon_\Omega = 1 \times 10^{-5}$					
	γ_{l_1}	Δt (s)	#split	#subset	gap	ϵ_h -opt?	γ_{l_2}	Δt (s)	#split	#subset	gap	ϵ_h -opt?
5×10^{-1}	11.571	0.966	65	42	0.1629	✓	11.673	0.195	8	9	2.4476	✗
1×10^{-1}	11.561	9.196	229	87	0.0337	✓	11.670	2.872	167	155	1.3510	✗
5×10^{-2}	11.560	7.433	289	85	0.0171	✓	11.615	3.925	257	173	0.7310	✗
1×10^{-2}	11.559	9.119	446	107	0.0038	✓	11.564	10.61	540	148	0.0996	✗
5×10^{-3}	11.559	8.371	499	109	0.0021	✓	11.560	17.5	768	181	0.0464	✗
1×10^{-3}	11.559	10.18	675	97	0.0005	✓	11.559	49.0	1621	408	0.0113	✗
5×10^{-4}	11.559	13.38	746	91	0.0003	✓	11.559	49.07	1760	403	0.0056	✗
1×10^{-4}	11.559	57.16	1921	229	0.0001	✗	11.559	71.27	1933	670	0.0014	✗
5×10^{-5}	11.559	42.06	1928	230	0.0001	✗	11.559	69.49	1997	670	0.0007	✗
1×10^{-5}	11.559	43.37	1943	231	0.0001	✗	11.559	36.69	1943	231	0.0001	✗

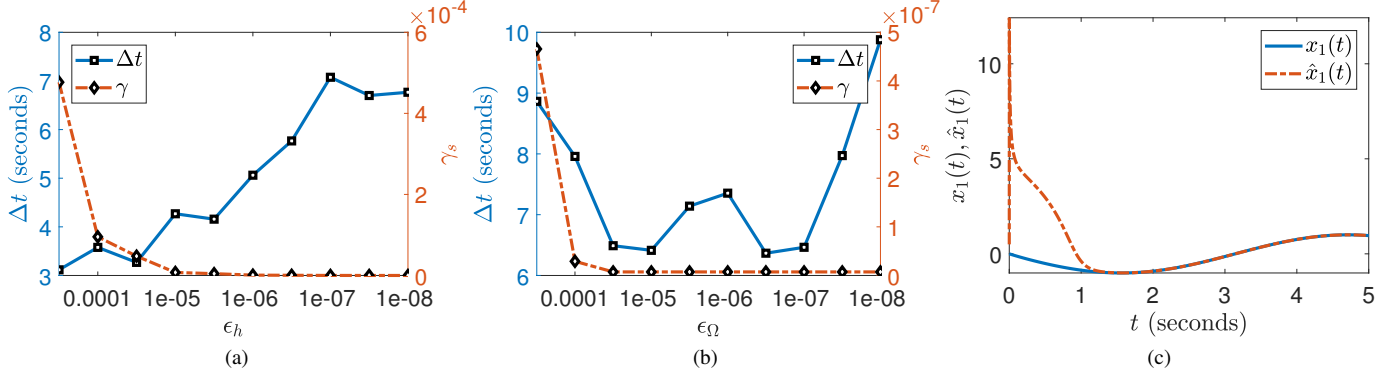


Figure 4. Numerical test results for dynamics of a moving object: (a) computational time (Δt) and one-sided Lipschitz constant (γ_s) for various ϵ_h , (b) the corresponding results for various ϵ_Ω , and (c) the trajectories of actual $x_1(t)$ and estimated $\hat{x}_1(t)$ state with $\gamma_s = 0$, $\gamma_{q1} = 25015$, and $\gamma_{q2} = -9999.89$.

constants using (7b) is considerably longer than using (8). Moreover, the computational time for Case 1 in increasing as M increases. This observation is in contrast to the results from Case 2—the computational time is somehow not affected by traffic dimension M since (a) only variables that appear on the expression of (28) are considered and (b) we only solve $\max_{\mathbf{x} \in \Omega} \|\nabla_{\mathbf{x}} f_c(\mathbf{x})\|_2^2$ once.

B. Lipschitz Parameterization for Synchronous Generator

The synchronous generator model considered in this example is taken from [22], which is a fourth-order differential equation where the dynamics are detailed in [22] with $\mathbf{f} : \mathbb{R}^4 \times \mathbb{R}^4 \rightarrow \mathbb{R}^4$ is comprised of the following form

$$\mathbf{f}_1(\mathbf{x}, \mathbf{u}) = -\alpha_1 \quad (30a)$$

$$\begin{aligned} \mathbf{f}_2(\mathbf{x}, \mathbf{u}) = & \alpha_3 x_4 u_4 \cos x_1 - \alpha_3 x_3 u_4 \sin x_1 - \alpha_3 x_4 u_3 \sin x_1 \\ & - \alpha_3 x_3 u_3 \cos x_1 + \alpha_4 u_3 u_4 \cos 2x_1 \\ & + \frac{1}{2} \alpha_4 (u_4^2 - u_3^2) \sin 2x_1 + \alpha_6 \end{aligned} \quad (30b)$$

$$\mathbf{f}_3(\mathbf{x}, \mathbf{u}) = \alpha_8 u_4 \cos x_1 - \alpha_8 u_3 \sin x_1 \quad (30c)$$

$$\mathbf{f}_4(\mathbf{x}, \mathbf{u}) = \alpha_{10} u_3 \cos x_1 + \alpha_{10} u_4 \sin x_1, \quad (30d)$$

where $\alpha_1, \alpha_3, \alpha_4, \alpha_6, \alpha_8$, and α_{10} are constants detailed in [22], \mathbf{x} is the state vector, and \mathbf{u} is the input vector such that

$$\mathbf{x} = [x_1 \ x_2 \ x_3 \ x_4]^\top = [\delta \ \omega \ e'_q \ e'_d]^\top$$

$$\mathbf{u} = [u_1 \ u_2 \ u_3 \ u_4]^\top = [T_m \ E_{fd} \ i_R \ i_I]^\top,$$

where δ is the rotor angle, ω is the rotor speed, and e'_q and e'_d are the transient voltage along q and d axes, T_m is the mechanical torque, E_{fd} is the internal field voltage, i_R and i_I are the real and imaginary currents of the generator [50]. In this case we consider a 16-machine, 68-bus system that is extracted from the

PST toolbox [51] by considering Generator 14 in the network, in which the corresponding parameters are obtained from [51]. The generator's dynamic response are generated from applying a three-phase fault at bus 6 of line 6–11 where each generator is using a transient model with IEEE Type DC1 excitation system and a simplified turbine-governor system [52]. To obtain lower and upper bounds on the state and input (which are needed to construct Ω), we measure their maxima and minima of the dynamic response within a 10 seconds time frame. We use the expression from (8) to compute Lipschitz constants together with formulations presented in [38] to find the corresponding intervals for sinusoidal functions.

The objectives of this numerical test are twofold. Firstly, we want to find the relation between the values of computed Lipschitz constant and computational time with different precision used in executing Algorithm 1 which is done by assigning different values for ϵ_h and ϵ_Ω . Secondly, we are interested in investigating the practical usefulness of the computed Lipschitz constant for actual observer design. The results of this test are summarized in Tab. IV. To comply with the first objective, two scenarios are considered: first, the value for ϵ_h is fixed while changing the value of ϵ_Ω and second we consider the other way, i.e., fixing ϵ_Ω while using different values for ϵ_h . From this table we see that, in both scenarios, the computed Lipschitz constant is decreasing and seems to converge to a value around 11.559 as ϵ_h and ϵ_Ω getting smaller. From this result we can conclude that a better Lipschitz constant can be obtained with better precision, i.e., smaller ϵ_h and ϵ_Ω , albeit in the expense of increasing computational time—see Figs. 3a and 3b. We also observe from Tab. IV that some solutions are actually *not* ϵ_h -optimal, since

the optimality gaps are indeed greater than the predefined ϵ_h . In comparison with the analytical Lipschitz constant computed using the formula described in [22] which is equal to 238.1831, the Lipschitz constant obtained using the proposed approach is far less conservative, therefore showcasing one particular advantage of the proposed approach together with its potential applicability for various observer/controller/observer-based stabilization designs for Lipschitz NDS. Finally, to answer the second objective, we use the computed Lipschitz constant $\gamma = 11.559$ and implement a Lipschitz-based observer for NDS developed in [1] for performing dynamic state estimation on this generator. We find that, with the given Lipschitz constant, the computed observer gain matrix is able to provide a converging estimation error. This finding is corroborated by the converging estimated generator rotor speed ω , denoted by $\hat{x}_2(t)$, to the actual one $x_2(t)$, as illustrated in Fig. 3c. This demonstrates the applicability of the proposed approach for practical observer design and state estimation.

C. OSL and QiB Parameterization

In the final numerical example, we consider the equation that represents the motion of a moving object in 2-D plane given in [4] and described in the following state-space equation

$$\dot{\mathbf{x}} = \begin{bmatrix} 1 & -1 \\ 1 & 1 \end{bmatrix} \mathbf{x} + \begin{bmatrix} -x_1(x_1^2 + x_2^2) \\ -x_2(x_1^2 + x_2^2) \end{bmatrix}, \quad \mathbf{y} = \begin{bmatrix} 0 & 1 \end{bmatrix} \mathbf{x}, \quad (31)$$

with domain of interest $\Omega = \{\mathbf{x} \in \mathbb{R}^2 \mid x_i \in [-r, r], i = 1, 2\}$ where $r = 5$. Here we aim to (a) find the one-sided Lipschitz constant γ_s and quadratically inner-bounded constants γ_{q1} and γ_{q2} that are (b) useful for observer design. To that end, first we focus on finding γ_s using the method given in Proposition 2. The corresponding matrix $\Xi(\mathbf{x})$ for the nonlinear functions in (31) is of the form

$$\Xi(\mathbf{x}) = \begin{bmatrix} -3x_1^2 - x_2^2 & -2x_1x_2 \\ -2x_1x_2 & -x_1^2 - 3x_2^2 \end{bmatrix}.$$

Since $\Xi(\mathbf{x})$ in the above is already symmetric, then according to (15), γ_s can be computed as

$$\gamma_s = \max_{i \in \{1,2\}} \left(\max_{\mathbf{x} \in \Omega} \left(\Xi_{(i,i)} + \sum_{j \in \{1,2\} \setminus i} |\Xi_{(i,j)}| \right) \right). \quad (32)$$

In using Algorithm 1 to solve (32), we first fix ϵ_Ω to 10^{-8} and use various values for ϵ_h ranging from 5×10^{-4} to 10^{-8} then in turn, fix ϵ_h and use various values for ϵ_Ω . The results of this numerical example is illustrated in Figs. 4a and 4b. It can be seen from these figures that, as ϵ_h getting smaller, the value of γ_s is decreasing to a value near zero. Therefore, we conclude that the one-sided Lipschitz constant for this system is zero. This results corroborates the fact that, as proven in [4], the system is indeed globally one-sided Lipschitz with $\gamma_s = 0$.

Next, we put our attention on determining the quadratically inner-bounded constant. To obtain such constant, we solve the following problems using Algorithm 1

$$\begin{aligned} \underline{\gamma} &= \min_{i \in \{1,2\}} \left(\min_{\mathbf{x} \in \Omega} \left(\Xi_{(i,i)} - \sum_{j \in \{1,2\} \setminus i} |\Xi_{(i,j)}| \right) \right) \\ \gamma_m &= \max_{\mathbf{x} \in \Omega} \sum_{i \in \{1,2\}} \|\nabla_{\mathbf{x}} f_i(\mathbf{x})\|_2^2, \end{aligned}$$

in which we obtain $\underline{\gamma} = -150$ and $\gamma_m = 2.5 \times 10^4$. According to Proposition 4, for any $\epsilon_1, \epsilon_2 \in \mathbb{R}_+$, the quadratically inner-bounded constant can be constructed as $\gamma_{q2} = \epsilon_2 - \epsilon_1$ and $\gamma_{q1} = \epsilon_1 \gamma_s - \epsilon_2 \underline{\gamma} + \gamma_m$. By setting the constants $\epsilon_1 = 10^5$ and $\epsilon_2 = 10^{-1}$, we obtain $\gamma_{q1} = 25015$ and $\gamma_{q2} = -9999.89$. To test the applicability of the computed one-sided Lipschitz and quadratically inner-bounded constants for state estimation, we implement an observer developed in [6] using the computed constants, in which we are successfully able to get a converging estimation error. Fig. 4c depicts the trajectories of the first actual and estimated state for this system.

VI. SUMMARY AND FUTURE DIRECTIONS

To the best of our knowledge, this is the first thorough research effort that presents analytical and computational methods to parameterize NDS and various corresponding function sets. Specifically, we propose a unified framework for NDS parameterization for bounded Jacobian, Lipschitz continuous, one-sided Lipschitz, quadratically inner-bounded, and quadratically bounded function sets. Our contributions are (1) posing and analytically deriving the NDS parameterization as global maximization problems, (2) investigating an interval-based algorithm to solve such global maximization problems, and (3) showcasing the proposed methodology for performing parameterization for some NDS models in traffic and power networks. We offer various strategies for reducing the complexity in parameterizing NDS using the proposed interval-based global maximization algorithm.

The presented methods in this paper are not devoid of limitations; several future research directions are worthy of further investigation. In particular, there exist other classes of nonlinearities that are not considered in this paper such as *incremental quadratic nonlinearity* [53] and *generalized sector nonlinearity* [54]. Parameterizing NDS for these kind of nonlinearities will be studied in our future work. Finally, investigating the impact of obtaining function sets and bounding constants, through our proposed algorithms, on LMI/SDP feasibility for observer and controller design is another direction worthy of exploring.

REFERENCES

- [1] G. Phanomchoeng and R. Rajamani, "Observer design for lipschitz nonlinear systems using riccati equations," in *Proceedings of the 2010 American Control Conference*, June 2010, pp. 6060–6065.
- [2] D. Ichalal, B. Marx, S. Mammar, D. Maquin, and J. Ragot, "Observer for lipschitz nonlinear systems: mean value theorem and sector nonlinearity transformation," in *2012 IEEE International Symposium on Intelligent Control*. IEEE, 2012, pp. 264–269.
- [3] A. Zemouche and M. Boutayeb, "Observer design for lipschitz nonlinear systems: the discrete-time case," *IEEE Transactions on Circuits and Systems II: Express Briefs*, vol. 53, no. 8, pp. 777–781, 2006.
- [4] M. Abbaszadeh and H. J. Marquez, "Nonlinear observer design for one-sided lipschitz systems," in *Proceedings of the 2010 American Control Conference*, June 2010, pp. 5284–5289.
- [5] M. Benallouch, M. Boutayeb, and M. Zasadzinski, "Observer design for one-sided lipschitz discrete-time systems," *Systems & Control Letters*, vol. 61, no. 9, pp. 879–886, 2012.
- [6] W. Zhang, H. Su, H. Wang, and Z. Han, "Full-order and reduced-order observers for one-sided lipschitz nonlinear systems using riccati equations," *Communications in Nonlinear Science and Numerical Simulation*, vol. 17, no. 12, pp. 4968–4977, 2012.
- [7] G. Phanomchoeng and R. Rajamani, "The bounded jacobian approach to nonlinear observer design," in *Proceedings of the 2010 American Control Conference*, June 2010, pp. 6083–6088.

- [8] G. Phanomchoeng, R. Rajamani, and D. Piyabongkarn, "Nonlinear observer for bounded jacobian systems, with applications to automotive slip angle estimation," *IEEE Transactions on Automatic Control*, vol. 56, no. 5, pp. 1163–1170, May 2011.
- [9] Y. Wang, R. Rajamani, and A. Zemouche, "Multi-objective nonlinear observer design using bmis," in *2018 Annual American Control Conference (ACC)*, June 2018, pp. 1346–1351.
- [10] A. Zemouche and M. Boutayeb, "On lmi conditions to design observers for lipschitz nonlinear systems," *Automatica*, vol. 49, no. 2, pp. 585–591, 2013.
- [11] M. Jin, H. Feng, and J. Lavaei, "Multiplier-based observer design for large-scale lipschitz systems," 2018.
- [12] D. D. Siljak and D. M. Stipanovic, "Robust stabilization of nonlinear systems: The lmi approach," *Mathematical Problems in Engineering*, vol. 6, no. 5, pp. 461–493, 2000.
- [13] D. D. Siljak, D. M. Stipanovic, and A. I. Zecevic, "Robust decentralized turbine/governor control using linear matrix inequalities," *IEEE Transactions on Power Systems*, vol. 17, no. 3, pp. 715–722, Aug 2002.
- [14] M. Yadegar, A. Afshar, and M. Davoodi, "Observer-based tracking controller design for a class of lipschitz nonlinear systems," *Journal of Vibration and Control*, vol. 24, no. 11, pp. 2112–2119, 2018.
- [15] A. Zemouche, R. Rajamani, H. Kheloufi, and F. Bedouhene, "Robust observer-based stabilization of lipschitz nonlinear uncertain systems via lmis-discussions and new design procedure," *International Journal of Robust and Nonlinear Control*, vol. 27, no. 11, pp. 1915–1939, 2017.
- [16] M. Ekrastian, "Observer-based controller for lipschitz nonlinear systems," *International Journal of Systems Science*, vol. 48, no. 16, pp. 3411–3418, 2017.
- [17] J. Song and S. He, "Robust finite-time h_∞ control for one-sided lipschitz nonlinear systems via state feedback and output feedback," *Journal of the Franklin Institute*, vol. 352, no. 8, pp. 3250–3266, 2015.
- [18] L. Liu and X. Song, "Static output tracking control of nonlinear systems with one-sided lipschitz condition," *Mathematical Problems in Engineering*, vol. 2014, 2014.
- [19] A. Rastegari, M. M. Arefi, and M. H. Asemani, "Robust h_∞ sliding mode observer-based fault-tolerant control for one-sided lipschitz nonlinear systems," *Asian Journal of Control*, vol. 21, no. 1, pp. 114–129, 2019.
- [20] H. Gholami and T. Binazadeh, "Observer-based h_∞ finite-time controller for time-delay nonlinear one-sided lipschitz systems with exogenous disturbances," *Journal of Vibration and Control*, vol. 25, no. 4, pp. 806–819, 2019.
- [21] M. Fazlyab, A. Robey, H. Hassani, M. Morari, and G. J. Pappas, "Efficient and accurate estimation of lipschitz constants for deep neural networks," *CoRR*, vol. abs/1906.04893, 2019.
- [22] S. A. Nugroho, A. F. Taha, and J. Qi, "Characterizing the nonlinearity of power system generator models," in *2019 American Control Conference (ACC)*. IEEE, July 2019, pp. 1936–1941.
- [23] G. Wood and B. Zhang, "Estimation of the lipschitz constant of a function," *Journal of Global Optimization*, vol. 8, no. 1, pp. 91–103, 1996.
- [24] R. Paulavičius and J. Žilinskas, "Analysis of different norms and corresponding lipschitz constants for global optimization," *Technological and Economic Development of Economy*, vol. 12, no. 4, pp. 301–306, 2006.
- [25] M. S. Darup and M. Mönnigmann, "Fast computation of lipschitz constants on hyperrectangles using sparse codelists," *Computers and Chemical Engineering*, vol. 116, pp. 135 – 143, 2018.
- [26] A. Chakrabarty, D. K. Jha, G. T. Buzzard, Y. Wang, and K. G. Vamvoudakis, "Safe approximate dynamic programming via kernelized lipschitz estimation," *IEEE Transactions on Neural Networks and Learning Systems*, pp. 1–15, 2020.
- [27] S. A. Nugroho, V. Hoang, M. Radosz, S. Wang, and A. F. Taha, "New Insights on One-Sided Lipschitz and Quadratically Inner-Bounded Nonlinear Dynamic Systems," in *The 2020 American Control Conference, Denver, Colorado*, 2020. [Online]. Available: <https://arxiv.org/pdf/2002.02361.pdf>
- [28] M. Abbaszadeh and H. J. Marquez, "Design of nonlinear state observers for one-sided lipschitz systems," *CoRR*, vol. abs/1302.5867, 2013. [Online]. Available: <http://arxiv.org/abs/1302.5867>
- [29] W. Trench, *Introduction to Real Analysis*. Prentice Hall/Pearson Education, 2003.
- [30] H. Márquez, *Nonlinear Control Systems: Analysis and Design*.
- [31] H. Khalil, *Nonlinear Systems*, ser. Pearson Education. Prentice Hall, 2002.
- [32] R. Horn and C. Johnson, *Matrix Analysis*. Cambridge University Press, 2013.
- [33] I. Bárány and J. Solymosi, "Gershgorin disks for multiple eigenvalues of non-negative matrices," in *A Journey Through Discrete Mathematics*. Springer, 2017, pp. 123–133.
- [34] Y. Guo, Y. Chen, and C. Zhang, "Decentralized state-observer-based traffic density estimation of large-scale urban freeway network by dynamic model," *Information*, vol. 8, no. 3, 2017.
- [35] A. Alessandri, "Design of observers for lipschitz nonlinear systems using lmi," *IFAC Proceedings Volumes*, vol. 37, no. 13, pp. 459 – 464, 2004, 6th IFAC Symposium on Nonlinear Control Systems 2004 (NOLCOS 2004), Stuttgart, Germany, 1-3 September, 2004.
- [36] Y. Guo, Y. Chen, and C. Zhang, "Decentralized state-observer-based traffic density estimation of large-scale urban freeway network by dynamic model," *Information*, vol. 8, no. 3, p. 95, 2017.
- [37] B. Moa, "Interval methods for global optimization," Ph.D. dissertation, University of Victoria, 2007.
- [38] M. Daumas, D. Lester, and C. Munoz, "Verified real number calculations: A library for interval arithmetic," *IEEE Transactions on Computers*, vol. 58, no. 2, pp. 226–237, 2009.
- [39] R. E. Moore, R. B. Kearfott, and M. J. Cloud, *Introduction to Interval Analysis*. Philadelphia, PA, USA: Society for Industrial and Applied Mathematics, 2009.
- [40] E. Hansen and G. Walster, *Global Optimization Using Interval Analysis: Revised And Expanded*. CRC Press, 2003.
- [41] K. Ichida and Y. Fujii, "An interval arithmetic method for global optimization," *Computing*, vol. 23, no. 1, pp. 85–97, 1979.
- [42] E. Van Kampen, "Global optimization using interval analysis: Interval optimization for aerospace applications," Ph.D. dissertation, Delft University of Technology, 2010.
- [43] M. Van Emden and B. Moa, "Termination criteria in the moore-skelboe algorithm for global optimization by interval arithmetic," in *Frontiers in Global Optimization*. Springer, 2004, pp. 585–597.
- [44] J. Löfberg, "YALMIP: A toolbox for modeling and optimization in matlab," in *Proc. IEEE Int. Symp. Computer Aided Control Syst. Design*, 2004, pp. 284–289.
- [45] E. D. Andersen and K. D. Andersen, "The mosek interior point optimizer for linear programming: an implementation of the homogeneous algorithm," in *High performance optimization*. Springer, 2000, pp. 197–232.
- [46] S. A. Nugroho, A. F. Taha, and C. Claudel, "Traffic density modeling and estimation on stretched highways: The case for lipschitz-based observers," in *2019 American Control Conference (ACC)*. IEEE, July 2019, pp. 2658–2663.
- [47] B. Greenshields, W. Channing, H. Miller *et al.*, "A study of traffic capacity," in *Highway research board proceedings*, vol. 1935. National Research Council (USA), Highway Research Board, 1935.
- [48] S. A. Nugroho, A. F. Taha, and C. G. Claudel, "A control-theoretic approach for scalable and robust traffic density estimation using convex optimization," *IEEE Transactions on Intelligent Transportation Systems*, pp. 1–15, 2019.
- [49] S. Contreras, P. Kachroo, and S. Agarwal, "Observability and sensor placement problem on highway segments: A traffic dynamics-based approach," *IEEE Transactions on Intelligent Transportation Systems*, vol. 17, no. 3, pp. 848–858, 2016.
- [50] P. Kundur, N. J. Balu, and M. G. Lauby, *Power system stability and control*. McGraw-hill New York, 1994, vol. 7.
- [51] J. H. Chow and K. W. Cheung, "A toolbox for power system dynamics and control engineering education and research," *Power Systems, IEEE Transactions on*, vol. 7, no. 4, pp. 1559–1564, 1992.
- [52] J. Qi, A. F. Taha, and J. Wang, "Comparing kalman filters and observers for power system dynamic state estimation with model uncertainty and malicious cyber attacks," *IEEE Access*, vol. 6, pp. 77 155–77 168, 2018.
- [53] B. Açikmeşe and M. Corless, "Observers for systems with nonlinearities satisfying incremental quadratic constraints," *Automatica*, vol. 47, no. 7, pp. 1339 – 1348, 2011.
- [54] K. Vijayaraghavan, "Observer design for generalized sector-bounded noisy nonlinear systems," *Proceedings of the Institution of Mechanical Engineers, Part I: Journal of Systems and Control Engineering*, vol. 228, no. 9, pp. 645–657, 2014.
- [55] R. Wu, W. Zhang, F. Song, Z. Wu, and W. Guo, "Observer-based stabilization of one-sided lipschitz systems with application to flexible link manipulator," *Advances in Mechanical Engineering*, vol. 7, no. 12, p. 1687814015619555, 2015.

APPENDIX A

OBSERVER, CONTROLLER, AND OBSERVER-BASED STABILIZATION FOR DIFFERENT CLASSES OF NDS

Table VI summarizes several type of observer design procedure via LMI for NDS which nonlinearities satisfy one of the following condition: bounded Jacobian, Lipschitz continuous, one-sided Lipschitz, and quadratically inner-bounded. Table V shows some controller and observer-based stabilization design via LMI for NDS with such nonlinearities.

Table V
CONTROLLER AND OBSERVER-BASED STABILIZATION DESIGNS FOR NDS WITH DIFFERENT CLASSES OF NONLINEARITY THROUGH SDPs OR LMIs [13], [14], [55].

Dynamics and Nonlinearity Class	Control/Observer Structures	Control Design via LMI
$\dot{x} = Ax + Gf(x) + Bu$ Quadratically Bounded: $\langle f(x), f(x) \rangle \leq x^\top H^\top H x$	$u = Kx$ $K = LP^{-1}$ Variables: P, L, γ	$\min \gamma$ s.t. $\begin{bmatrix} AP + PA^\top + BL + L^\top B^\top & * & * \\ G^\top & -I & * \\ HP & O & -\gamma I \end{bmatrix} \prec 0,$ $P \succ 0, \gamma > 0$
$\dot{x} = Ax + f(x) + Bu$ Glob./Loc. Lipschitz: $\ f(x) - f(\hat{x})\ _2 \leq \gamma_l \ x - \hat{x}\ _2$	$u = -Kx$ $K = WQ^{-1}$ Variables: Q, W Constant: $\rho > 0$	find $Q \succ 0, W$ s.t. $\begin{bmatrix} AQ + QA^\top - BW - W^\top B^\top + \frac{1}{\rho} I & * \\ Q & -\frac{1}{\rho \gamma_l^2} I \end{bmatrix} \prec 0,$
$\dot{x} = Ax + f(x) + Bu$ $y = Cx$ One-Sided Lipschitz, Quadratically Bounded: constants $\gamma_s, \gamma_{q1}, \gamma_{q2}$ (see Tab. I)	$\dot{\hat{x}} = A\hat{x} + f(\hat{x}) + Bu$ $\hat{y} = C\hat{x}$ $u = F\hat{x}$ $K = R^{-1}\hat{K}^\top$ $F = \hat{F}^\top Q^{-1}$ Variables: Q, R, \hat{K}, \hat{F} , $\epsilon_1, \epsilon_2, \epsilon_3, \epsilon_4$ Constant: $\phi_1 > 0$	find $Q \succ 0, R \succ 0, \hat{K}, \hat{F}, \epsilon_1 > 0, \epsilon_2 > 0, \epsilon_3 > 0, \epsilon_4 > 0$ s.t. $\begin{bmatrix} S_1 & * \\ S_2^\top & S_3 \end{bmatrix} \prec 0$ $S_1 = \begin{bmatrix} \tilde{\Sigma}_{11}(Q, \hat{F}) & * & * & * \\ O & \tilde{\Sigma}_{22}(R, \hat{K}, \epsilon_3, \epsilon_4, \gamma_s, \gamma_{q1}) & * & * \\ I & O & -2\epsilon_2 I & * \\ O & R + (\epsilon_4 \gamma_{q2} - \epsilon_3) I & O & -2\epsilon_4 I \end{bmatrix}$ $S_2 = \begin{bmatrix} -B\hat{F}^\top & O & Q & O \\ O & I & O & O \\ O & O & O & I \\ O & O & O & O \end{bmatrix}$ $S_3 = \text{Diag} \left(\begin{bmatrix} -\frac{Q}{\phi_1} & -\phi_1 Q & -\psi(\epsilon_1, \epsilon_2) I & -\zeta(\epsilon_1, \epsilon_2) I \end{bmatrix} \right)$

Table VI
OBSERVER DESIGNS FOR NDS WITH DIFFERENT CLASSES OF NONLINEARITY THROUGH SDPs OR LMIs [1], [6], [11], [48].

Dynamics and Nonlinearity Class	Observer Structures	Observer Design via LMI
$\dot{\mathbf{x}} = \mathbf{A}\mathbf{x} + \mathbf{f}(\mathbf{x}) + \mathbf{B}\mathbf{u}$ $\mathbf{y} = \mathbf{C}\mathbf{x} + \mathbf{D}\mathbf{u}$ Glob/Loc. Lipschitz: $\ \mathbf{f}(\mathbf{x}) - \mathbf{f}(\hat{\mathbf{x}})\ _2 \leq \gamma_l \ \mathbf{x} - \hat{\mathbf{x}}\ _2$	$\dot{\hat{\mathbf{x}}} = \mathbf{A}\hat{\mathbf{x}} + \mathbf{f}(\hat{\mathbf{x}}) + \mathbf{B}\mathbf{u}$ $\quad + \mathbf{L}(\mathbf{y} - \hat{\mathbf{y}})$ $\hat{\mathbf{y}} = \mathbf{C}\hat{\mathbf{x}} + \mathbf{D}\mathbf{u}$ $\mathbf{L} = \mathbf{P}^{-1}\mathbf{Y}$ Variables: $\mathbf{P}, \mathbf{Y}, \kappa$	find $\mathbf{P} \succ 0, \mathbf{Y}, \kappa > 0$ s.t. $\begin{bmatrix} \mathbf{A}^\top \mathbf{P} + \mathbf{P}\mathbf{A} - \mathbf{Y}\mathbf{C} & & \\ -\mathbf{C}^\top \mathbf{Y}^\top + \kappa \gamma_l^2 \mathbf{I} & * & \\ \mathbf{P} & & -\kappa \mathbf{I} \end{bmatrix} \prec 0,$
$\dot{\mathbf{x}} = \mathbf{A}\mathbf{x} + \mathbf{G}\mathbf{f}(\mathbf{x}) + \mathbf{B}\mathbf{u}$ $\mathbf{y} = \mathbf{C}\mathbf{x} + \mathbf{D}\mathbf{u}$ One-Sided Lipschitz, Quadratically Inner-Bounded: constants $\gamma_s, \gamma_{q1}, \gamma_{q2}$ (see Tab. I)	$\dot{\hat{\mathbf{x}}} = \mathbf{A}\hat{\mathbf{x}} + \mathbf{G}\mathbf{f}(\hat{\mathbf{x}}) + \mathbf{B}\mathbf{u}$ $\quad + \mathbf{L}(\mathbf{y} - \hat{\mathbf{y}})$ $\hat{\mathbf{y}} = \mathbf{C}\hat{\mathbf{x}} + \mathbf{D}\mathbf{u}$ $\mathbf{L} = \frac{1}{2} \sigma \mathbf{P}^{-1} \mathbf{C}^\top$ Variables: $\mathbf{P}, \sigma, \epsilon_1, \epsilon_2$	find $\mathbf{P} \succ 0, \{\sigma, \epsilon_1, \epsilon_2\} > 0$ s.t. $\begin{bmatrix} \mathbf{A}^\top \mathbf{P} + \mathbf{P}\mathbf{A} + \epsilon_1 \gamma_s \mathbf{I} & & \\ + \epsilon_2 \gamma_{q1} \mathbf{I} - \sigma \mathbf{C}^\top \mathbf{C} & * & \\ \mathbf{G}^\top \mathbf{P} + \frac{\gamma_{q2} \epsilon_2 - \epsilon_1}{2} \mathbf{I} & & -\epsilon_2 \mathbf{I} \end{bmatrix} \prec 0$
$\dot{\mathbf{x}} = \mathbf{A}\mathbf{x} + \mathbf{B}_u \mathbf{u} + \mathbf{G}\mathbf{f}(\mathbf{x}) + \mathbf{B}_w \mathbf{w}$ $\mathbf{y} = \mathbf{C}\mathbf{x} + \mathbf{D}_u \mathbf{u} + \mathbf{D}_w \mathbf{w}$ Glob/Loc. Lipschitz: $\ \mathbf{f}(\mathbf{x}) - \mathbf{f}(\hat{\mathbf{x}})\ _2 \leq \gamma_l \ \mathbf{x} - \hat{\mathbf{x}}\ _2$	$\dot{\hat{\mathbf{x}}} = \mathbf{A}\hat{\mathbf{x}} + \mathbf{G}\mathbf{f}(\hat{\mathbf{x}}) + \mathbf{B}\mathbf{u}$ $\quad + \mathbf{L}(\mathbf{y} - \hat{\mathbf{y}})$ $\hat{\mathbf{y}} = \mathbf{C}\hat{\mathbf{x}} + \mathbf{D}_u \mathbf{u}$ $\mathbf{L} = \mathbf{P}^{-1}\mathbf{Y}$ Variables: $\mathbf{P}, \mathbf{Y}, \kappa, \mu_1, \mu_2$ Constant: $\alpha > 0$	min $\mu_1 + \mu_2$ s.t. $\begin{bmatrix} \mathbf{A}^\top \mathbf{P} + \mathbf{P}\mathbf{A} - \mathbf{Y}\mathbf{C} & & & \\ -\mathbf{C}^\top \mathbf{Y}^\top + \kappa \gamma_l^2 \mathbf{I} + \alpha \mathbf{P} & * & * & \\ \mathbf{G}^\top \mathbf{P} & & -\kappa \mathbf{I} & * \\ \mathbf{B}_w^\top \mathbf{P} - \mathbf{D}_w^\top \mathbf{Y}^\top & & \mathbf{O} & -\alpha \mu_1 \mathbf{I} \end{bmatrix} \prec 0$ $\begin{bmatrix} -\mathbf{P} & * & * \\ \mathbf{O} & -\mu_2 \mathbf{I} & * \\ \mathbf{Z} & \mathbf{O} & -\mathbf{I} \end{bmatrix} \prec 0$ $\mathbf{P} \succ 0, \mathbf{Y}, \{\kappa, \mu_1, \mu_2\} > 0$
$\dot{\mathbf{x}} = \mathbf{A}\mathbf{x} + \mathbf{G}\mathbf{f}(\mathbf{x}) + \mathbf{B}\mathbf{u}$ $\mathbf{y} = \mathbf{C}\mathbf{x} + \mathbf{D}\mathbf{u}$ Bounded Jacobian: $\underline{\mathbf{f}} \leq \mathbf{D}_x \mathbf{f}(\mathbf{x}) \leq \bar{\mathbf{f}}$ $\underline{b}_{ij} := \underline{f}_{(i,j)}, \bar{b}_{ij} := \bar{f}_{(i,j)}$	$\dot{\hat{\mathbf{x}}} = \mathbf{A}\hat{\mathbf{x}} + \mathbf{G}\mathbf{f}(\hat{\mathbf{x}}) + \mathbf{B}\mathbf{u}$ $\quad + \mathbf{L}(\mathbf{y} - \hat{\mathbf{y}})$ $\hat{\mathbf{y}} = \mathbf{C}\hat{\mathbf{x}} + \mathbf{D}\mathbf{u}$ $\mathbf{L} = \mathbf{P}^{-1}\mathbf{Y}$ Variables: $\mathbf{P}, \mathbf{Y}, \Lambda$ Constants: $\underline{c}_{ij} = \frac{1}{2} (\underline{b}_{ij} + \bar{b}_{ij}), \forall i, j$ $\bar{c}_{ij} = \frac{1}{2} (\underline{b}_{ij} - \bar{b}_{ij}), \forall i, j$ $\mathbf{W} = \mathbf{I}_g \otimes \mathbf{1}_{1 \times n_x}$	find $\mathbf{P} \succ 0, \mathbf{Y}, \Lambda$ s.t. $\begin{bmatrix} \mathbf{A}^\top \mathbf{P} + \mathbf{P}\mathbf{A} - \mathbf{Y}\mathbf{C} & & \\ -\mathbf{C}^\top \mathbf{Y}^\top + \Theta_1(\Lambda) & * & \\ \mathbf{W}^\top \mathbf{G}^\top \mathbf{P} + \Theta_2(\Lambda) & & \Theta_3(\Lambda) \end{bmatrix} \prec 0$ $\Theta_1(\Lambda) = \text{Diag} \left(\left\{ \sum_{i=1}^n \lambda_{ij} (\bar{c}_{ij}^2 - \underline{c}_{ij}^2) \right\}_{j=1}^n \right)$ $\Theta_2(\Lambda)^\top = \left[\left\{ \text{Diag}([\lambda_{i1} \underline{c}_{i1}, \dots, \lambda_{in_x} \underline{c}_{in_x}]) \right\}_{i=1}^n \right]$ $\Theta_3(\Lambda) = \text{Diag}(\text{vec}(\Lambda))$